

AD-A180 358

EXPERIMENTS ON LEARNING BY BACK PROPAGATION(U)
CARNEGIE-MELLON UNIV PITTSBURGH PA DEPT OF COMPUTER
SCIENCE D C PLAUT ET AL. JUN 86 CMU-CS-86-126

1/1

UNCLASSIFIED

NO0014-86-K-0167

P/G 12/9

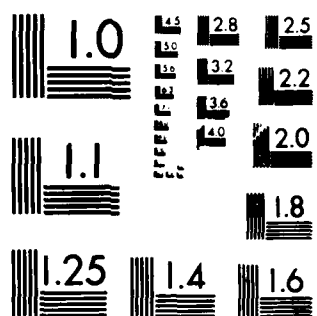
NL

END

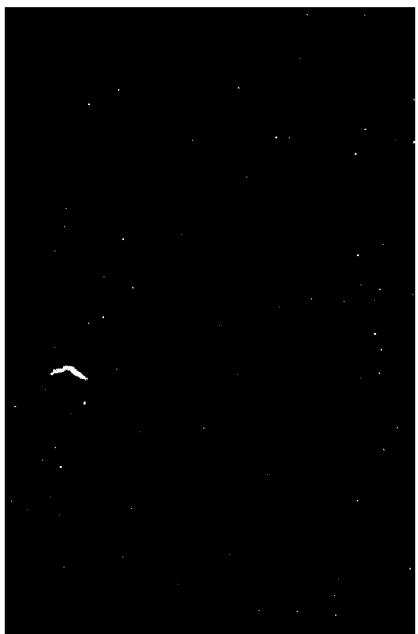
DATE

FILED

5 87



MICROCOPY RESOLUTION TEST CHART
NATIONAL BUREAU OF STANDARDS-1963-A



UNCLASSIFIED
SECURITY CLASSIFICATION OF THIS PAGE

ADA18358

REPORT DOCUMENTATION PAGE				Form Approved OMB No. 0704-0188	
1a. REPORT SECURITY CLASSIFICATION Unclassified			1b. RESTRICTIVE MARKINGS		
2a. SECURITY CLASSIFICATION AUTHORITY			3. DISTRIBUTION / AVAILABILITY OF REPORT Approved for public release; distribution unlimited		
2b. DECLASSIFICATION / DOWNGRADING SCHEDULE					
4. PERFORMING ORGANIZATION REPORT NUMBER(S) CMU-CS-86-126			5. MONITORING ORGANIZATION REPORT NUMBER(S)		
6a. NAME OF PERFORMING ORGANIZATION Carnegie-Mellon University		6b. OFFICE SYMBOL (if applicable)	7a. NAME OF MONITORING ORGANIZATION Personnel and Training Research Programs Office of Naval Research		
6c. ADDRESS (City, State, and ZIP Code) Department of Computer Science Pittsburgh, PA 15213			7b. ADDRESS (City, State, and ZIP Code) 800 North Quincy Street Arlington, VA 22217-5000		
8a. NAME OF FUNDING / SPONSORING ORGANIZATION		8b. OFFICE SYMBOL (if applicable)	9. PROCUREMENT INSTRUMENT IDENTIFICATION NUMBER N00014-86-K-0167		
8c. ADDRESS (City, State, and ZIP Code)			10. SOURCE OF FUNDING NUMBERS		
			PROGRAM ELEMENT NO. 61153N	PROJECT NO. RR04206	TASK NO. RR04206-0B
			WORK UNIT ACCESSION NO. 442b-467		
11. TITLE (Include Security Classification) Experiments on learning by back propagation					
12. PERSONAL AUTHOR(S) Plaut, David C., Nowlan, Steven, J., & Hinton, Geoffrey E.					
13a. TYPE OF REPORT Technical		13b. TIME COVERED FROM _____ TO _____		14. DATE OF REPORT (Year, Month, Day) Apr 11 28, 1987	
				15. PAGE COUNT June 86	
16. SUPPLEMENTARY NOTATION					
17. COSATI CODES			18. SUBJECT TERMS (Continue on reverse if necessary and identify by block number)		
FIELD	GROUP	SUB-GROUP			
			Learning; connectionist networks; error propagation; neural modeling		
19. ABSTRACT (Continue on reverse if necessary and identify by block number)					
OVER					
20. DISTRIBUTION / AVAILABILITY OF ABSTRACT <input type="checkbox"/> UNCLASSIFIED/UNLIMITED <input checked="" type="checkbox"/> SAME AS RPT <input type="checkbox"/> DTIC USERS			21. ABSTRACT SECURITY CLASSIFICATION Unclassified		
22a. NAME OF RESPONSIBLE INDIVIDUAL Dr. Harold Hawkins			22b. TELEPHONE (Include Area Code) 202-696-4323		22c. OFFICE SYMBOL 1142PT

Abstract

Rumelhart, Hinton and Williams [Rumelhart 86] describe a learning procedure for layered networks of deterministic, neuron-like units. This paper describes further research on the learning procedure. We start by describing the units, the way they are connected, the learning procedure, and the extension to iterative nets. We then give an example in which a network learns a set of filters that enable it to discriminate formant-like patterns in the presence of noise.

The speed of learning is strongly dependent on the shape of the surface formed by the error measure in "weight space." We give examples of the shape of the error surface for a typical task and illustrate how an acceleration method speeds up descent in weight space.

The main drawback of the learning procedure is the way it scales as the size of the task and the network increases. We give some preliminary results on scaling and show how the magnitude of the optimal weight changes depends on the fan-in of the units. Additional results illustrate the effects on learning speed of the amount of interaction between the weights.

A variation of the learning procedure that back-propagates desired state information rather than error gradients is developed and compared with the standard procedure.

Finally, we discuss the relationship between our iterative networks and the "analog" networks described by Hopfield and Tank [Hopfield 85]. The learning procedure can discover appropriate weights in their kind of network, as well as determine an optimal schedule for varying the nonlinearity of the units during a search.

Table of Contents

1. Introduction	1
1.1. The Units	1
1.2. Layered Feed-forward Nets	2
1.3. The Learning Procedure	2
1.4. The Extension to Iterative Nets	4
2. Learning to Discriminate Noisy Signals	6
3. Characteristics of Weight Space	10
4. How the Learning Time Scales	19
4.1. Experiments	19
4.2. Unit Splitting	20
4.3. Varying Epsilon with Fan-In	21
5. Reducing the Interactions between the Weights	22
5.1. Experiments	22
5.2. Very fast learning with no generalization	23
6. Back Propagating Desired States	23
6.1. General Approach	24
6.2. Details	25
6.3. General Performance	25
6.4. Scaling Performance	26
6.5. Conclusions on Back Propagating Desired States	27
7. Gain Variation in Iterative Nets	27
7.1. Introduction	27
7.2. Implementation of Gain Variation	30
7.3. Experimental Results	31

Accession For	
NTIS	CRA&I <input checked="" type="checkbox"/>
ERIC	TAB <input type="checkbox"/>
Unannounced	<input type="checkbox"/>
Justification	
Report date correct	
By per phone con	
Distribution/	
Availability Codes	
Dist	Avail and/or Special
A-1	



1. Introduction

Rumelhart, Hinton and Williams [Rumelhart 86] describe a learning procedure for layered networks of deterministic, neuron-like units. The procedure repeatedly adjusts the weights in the network so as to minimize a measure of the difference between the actual output vector of the net and the desired output vector given the current input vector. This report describes further research on the learning procedure.

We start by describing the units, the way they are connected, the learning procedure, and the extension to iterative nets. We then give an example in which a network learns a set of filters that enable it to discriminate formant-like patterns in the presence of noise. The example shows how the learning procedure discovers weights that turn units in intermediate layers into an "ecology" of useful feature detectors each of which complements the other detectors.

The speed of learning is strongly dependent on the shape of the surface formed by the error measure in "weight space." This space has one dimension for each weight in the network and one additional dimension (height) that represents the overall error in the network's performance for any given set of weights. For many tasks, the error surface contains ravines that cause problems for simple gradient descent procedures. We give examples of the shape of the error surface for a typical task and illustrate the advantages of using an acceleration method to speed up progress down the ravine without causing divergent "sloshing" across the ravine.

The main drawback of the learning procedure is the way it scales as the size of the task and the network increases. We give some preliminary results on scaling and show how the magnitude of the optimal weight changes depends on the fan-in of the units. Additional results illustrate the effects on learning speed of the amount of interaction between the weights.

A variation of the learning procedure that back-propagates desired state information rather than error gradients is developed and compared with the standard procedure.

Finally, we discuss the relationship between our iterative networks and the "analog" networks described by Hopfield and Tank [Hopfield 85]. The learning procedure can be used to discover appropriate weights in their kind of network. It can also be used to determine an optimal schedule for varying the nonlinearity of the units during a search.

1.1. The Units

The total input, x_j , to unit j is a linear function of the outputs of the units, i , that are connected to j and of the weights, w_{ji} , on these connections.

$$x_j = \sum_i y_i w_{ji} \quad (1)$$

A unit has a real-valued output, y_j , that is a non-linear function of its total input.

$$y_j = \frac{1}{1 + e^{-x_j}} \quad (2)$$

It is not necessary to use exactly the functions given by Eqs. 1 and 2. Any input-output function that has a bounded

derivative will do. However, the use of a linear function for combining the inputs to a unit before applying the nonlinearity greatly simplifies the learning procedure.

1.2. Layered Feed-forward Nets

The simplest form of the learning procedure is for layered networks that have a layer of input units at the bottom, any number of intermediate layers, and a layer of output units at the top. Connections within a layer or from higher to lower layers are forbidden. The only connections allowed are ones from lower layers to higher layers, but the layers do not need to be adjacent; connections can skip layers.

An input vector is presented to the network by setting the states of the input units. Then the states of the units in each layer are determined by applying Eqs. 1 and 2 to the connections coming from lower layers. All units within a layer have their states set in parallel, but different layers have their states set sequentially, starting at the bottom and working upwards until the states of the output units are determined.

1.3. The Learning Procedure

The aim of the learning procedure is to find a set of weights which ensures that for each input vector the output vector produced by the network is the same as (or sufficiently close to) the desired output vector. If there is a fixed, finite set of input-output cases, the total error in the performance of the network with a particular set of weights can be computed by comparing the actual and desired output vectors for every case. The error, E , is defined by

$$E = \frac{1}{2} \sum_c \sum_j (y_{j,c} - d_{j,c})^2 \quad (3)$$

where c is an index over cases (input-output pairs), j is an index over output units, y is the actual state of an output unit, and d is its desired state. To minimize E by gradient descent it is necessary to compute the partial derivative of E with respect to each weight in the network. This is simply the sum of the partial derivatives for each of the input-output cases. For a given case, the partial derivatives of the error with respect to each weight are computed in two passes. We have already described the forward pass in which the units in each layer have their states determined by the input they receive from units in lower layers using Eqs. 1 and 2. The backward pass that propagates derivatives from the top layer back to the bottom one is more complicated.

The backward pass starts by computing $\frac{\partial E}{\partial y}$ for each of the output units. Differentiating Eq. 3 for a particular case, c , and suppressing the index c gives

$$\frac{\partial E}{\partial y_j} = y_j - d_j.$$

We can then apply the chain rule to compute $\frac{\partial E}{\partial x_j}$,

$$\frac{\partial E}{\partial x_j} = \frac{\partial E}{\partial y_j} \frac{dy_j}{dx_j}.$$

Differentiating Eq. 2 to get the value of $\frac{dy_j}{dx_j}$ gives

$$\frac{\partial E}{\partial x_j} = \frac{\partial E}{\partial y_j} y_j (1-y_j). \quad (4)$$

This means that we know how a change in the total input, x , to an output unit will affect the error. But this total input is just a linear function of the states of the lower level units and the weights on the connections, so it is easy to compute how the error will be affected by changing these states and weights. For a weight, w_{ji} , from i to j , the derivative is

$$\begin{aligned} \frac{\partial E}{\partial w_{ji}} &= \frac{\partial E}{\partial x_j} \cdot \frac{\partial x_j}{\partial w_{ji}} \\ &= \frac{\partial E}{\partial x_j} y_i \end{aligned} \quad (5)$$

and for the output of the i^{th} unit the contribution to $\frac{\partial E}{\partial y_i}$ resulting from the effect of i on j is simply

$$\frac{\partial E}{\partial x_j} \cdot \frac{\partial x_j}{\partial y_i} = \frac{\partial E}{\partial x_j} w_{ji}$$

so taking into account all the connections emanating from unit i we have

$$\frac{\partial E}{\partial y_i} = \sum_j \frac{\partial E}{\partial x_j} w_{ji}. \quad (6)$$

Figure 1-1 shows these steps of the backward pass laid out graphically. We have now seen how to compute $\frac{\partial E}{\partial y}$ for any unit in the penultimate layer when given $\frac{\partial E}{\partial y}$ for all units in the last layer. We can therefore repeat this procedure to compute $\frac{\partial E}{\partial y}$ for successively earlier layers, computing $\frac{\partial E}{\partial w}$ for the weights as we go. The amount of computation required for the backward pass is of the same order as the forward pass (it is linear in the number of connections) and the form of the computation is also similar. In both cases, the units compute a sum by multiplying each incoming quantity by the weight on the connection (see Eqs. 1 and 6). In the backward pass all the connections are used backwards, and $\frac{\partial E}{\partial y}$ plays the role that y plays in the forward pass. The main difference is that in the forward pass the sum is put through a nonlinear function, whereas in the backward pass it is simply multiplied by $y_j(1-y_j)$.

One way of using $\frac{\partial E}{\partial w}$ is to change the weights after every input-output case. This has the advantage that no separate memory is required for the derivatives. An alternative scheme, which we used in the research reported here, is to accumulate $\frac{\partial E}{\partial w}$ over all the input-output cases (or over a large number of them if it is not a finite set) before changing the weights.

The simplest version of gradient descent is to change each weight by an amount proportional to the accumulated $\frac{\partial E}{\partial w}$.

$$\Delta w = -\epsilon \frac{\partial E}{\partial w}.$$

This method does not converge as rapidly as methods that make use of the second derivatives, but it is much simpler and can easily be implemented by local computations in parallel hardware. It can be significantly improved, without sacrificing the simplicity and locality, by using an *acceleration* method in which the current gradient is used to

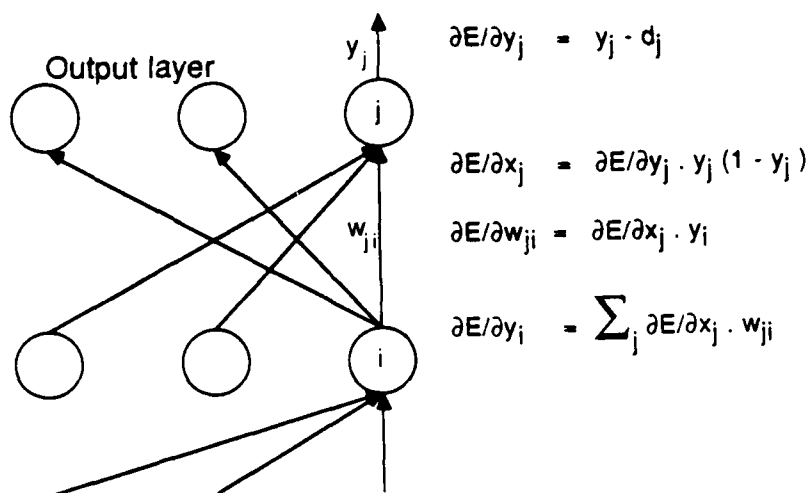


Figure 1-1: This shows the steps involved in computing $\partial E / \partial y$ for the intermediate layers of a multilayer network. The backward pass starts at the top of the figure and works downwards. Not all the connections are shown.

modify the velocity of the point in weight space instead of its position.

$$\Delta w(t) = -\epsilon \frac{\partial E}{\partial w(t)} + \alpha \Delta w(t-1) \quad (7)$$

where t is incremented by 1 for each sweep through the whole set of input-output cases (called an *epoch*), and α is an exponential decay factor between 0 and 1 (called *momentum*¹) that determines the relative contribution of the current and past gradients to the weight change. Eq. 7 can be viewed as describing the behavior of a ball-bearing rolling down the error surface when the whole system is immersed in a liquid with viscosity determined by α . The effectiveness of this acceleration method is discussed in Section 3.

The learning procedure is entirely deterministic, so if two units within a layer start off with the same connectivity and weights, there is nothing to make them ever differ from each other. We break this symmetry by starting with small random weights.

1.4. The Extension to Iterative Nets

Figure 1-2 shows the equivalence between an iterative net that is run synchronously for 3 iterations and a layered net in which each layer after the input corresponds to one iteration of the synchronous net. Using this equivalence, it is clear that we can always construct a layered net that will perform the same computation as an iterative net, provided we know the number of iterations in advance. Both nets have the same delay time between receiving the

¹We call α the momentum because that has appropriate physical connotations, even though this is not a precise analogy. The correct analogy is to viscosity. α is not equal to the viscosity, but it uniquely determines it.

input and giving the output.

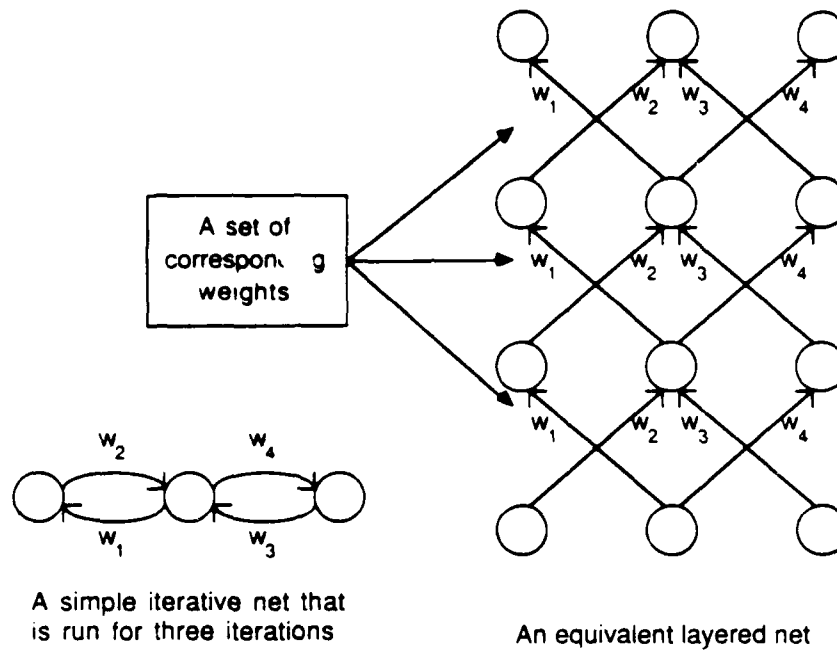


Figure 1-2: An iterative net and the equivalent layered net.

Since we have a learning procedure for layered nets, we could learn iterative computations by first constructing the equivalent layered net, then doing the learning, then converting back to the iterative net. Or we could avoid the construction by simply mapping the learning procedure itself into the form appropriate for the iterative net. Two complications arise in performing this conversion:

1. In a layered net the outputs of the units in the intermediate layers during the forward pass are required for performing the backward pass (see Eqs. 4 and 5). So in an iterative net it is necessary to store the output states of each unit that are temporally intermediate between the initial and final states.
2. For a layered net to be equivalent to an iterative net, corresponding weights between different layers must have the same value, as in figure 1-2. There is no guarantee that the basic learning procedure for layered nets will preserve this property. However, we can easily modify it by averaging $\partial E / \partial w$ for all the weights in each set of corresponding weights, and then changing each weight by an amount proportional to this average gradient. This is equivalent to taking the weight-change vector produced by the basic learning procedure and then projecting it onto the subspace of layered nets that are equivalent to iterative ones.

With these two provisos, the learning procedure can be applied directly to iterative nets and can be used to learn sequential structures. Several examples are given in [Rumelhart 86]. We return to iterative nets at the end of this paper and show how the learning procedure can be further modified to allow it to learn how to vary the nonlinearity in Eq. 2 as the network settles.

2. Learning to Discriminate Noisy Signals

Rumelhart, Hinton, and Williams [Rumelhart 86] illustrate the performance of the learning procedure on many different, simple tasks. We give a further example here which demonstrates that the procedure can construct sets of filters that are good at discriminating between rather similar signals in the presence of a lot of noise. We used an artificial task (suggested by Alex Waibel) which was intended to resemble a task that arises in speech recognition. We are currently working on extending this approach to real speech data.

The input is a synthetic spectrogram that represents the energy in six different frequency bands at nine different times. Figure 2-1 shows examples of spectrograms with no random variation in the level of the signal or the background, and figure 2-2 shows examples with added noise. The problem is to decide whether the signal is simply a horizontal track or whether it rises at the beginning. There is variation in both the frequency and onset time of the signal.

It is relatively easy to decide on the frequency of the horizontal part of the track, but it is much harder to distinguish the "risers" from the "non-risers" because the noise in the signal and background obscures the rise. To make the distinction accurately, the network needs to develop a set of filters that are carefully tuned to the critical differences. The filters must cover the range of possible frequencies and onset times, and when several different filters fit quite well, their outputs must be correctly weighted to give the right answer.

We used a network with three layers as shown in figure 2-3. Initially we tried training the network by repeatedly sweeping through a fixed set of 1000 examples, but the network learned to use the structure of the noise to help it discriminate the difficult cases, and so it did not generalize well when tested on new examples in which the noise was different. We therefore decided to generate a new example every time so that, in the long run, there were no spurious correlations between the noise and the signal. Because the network lacks a strong *a priori* model of the nature of the task, it has no way of telling the difference between a spurious correlation caused by using too small a sample and a systematic correlation that reflects the structure of the task.

Examples were generated by the following procedure:

1. Decide to generate a riser or a non-riser with equal probability.
2. If it is a non-riser pick one of the six frequencies at random. If it is a riser pick one of the four highest frequencies at random (the final frequency of a riser must be one of these four because it must rise through two frequency bands at the beginning).
3. Pick one of 5 possible onset times at random.
4. Give each of the input units a value of 0.4 if it is part of the signal and a value of 0.1 if it is part of the background. We now have a noise-free spectrogram of the kind shown in figure 2-1.
5. Add independent gaussian noise with mean 0 and standard deviation 0.15 to each unit that is part of the signal. Add independent gaussian noise with mean 0 and standard deviation 0.1 to the background. If any unit now has a negative activity level, set its level to 0.

The weights were modified after each block of 25 examples. For each weight, the values of $\frac{\partial E}{\partial w}$ were summed for all 25 cases and the weight increment after block t was given by Eq. 7. For the first 25 examples we used $\epsilon=0.005$ and $\alpha=0.5$. After this the weights changed rather slowly and the values were raised to $\epsilon=0.07$ and $\alpha=0.99$. We have found that it is generally helpful to use more conservative values at the beginning because the gradients are initially

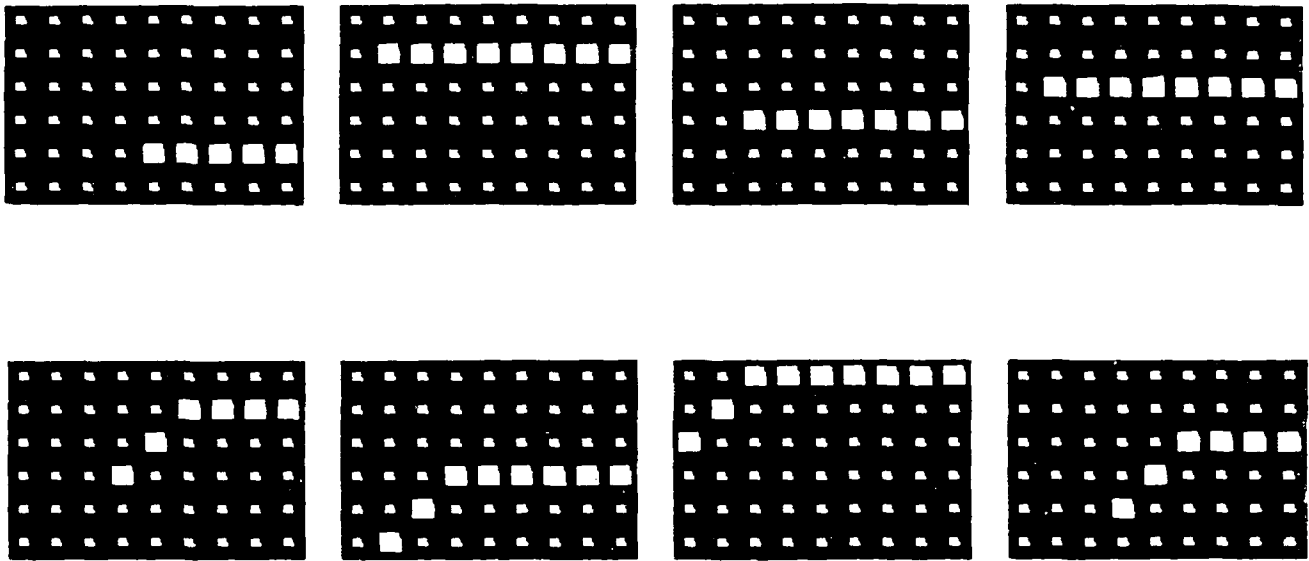


Figure 2-1: Synthetic spectrograms.

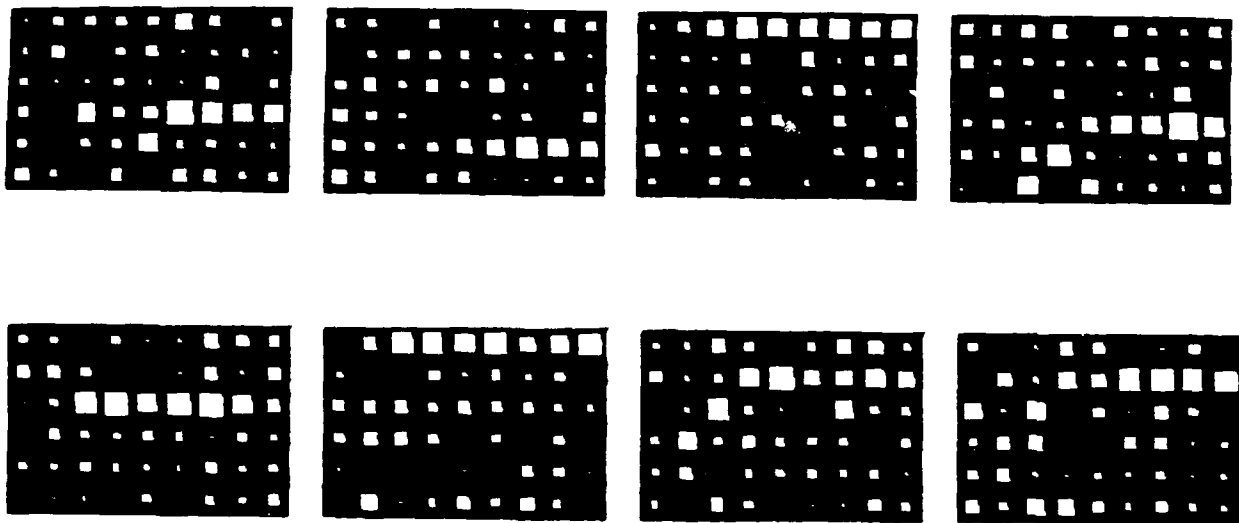


Figure 2-2: Synthetic spectrograms with random noise added.

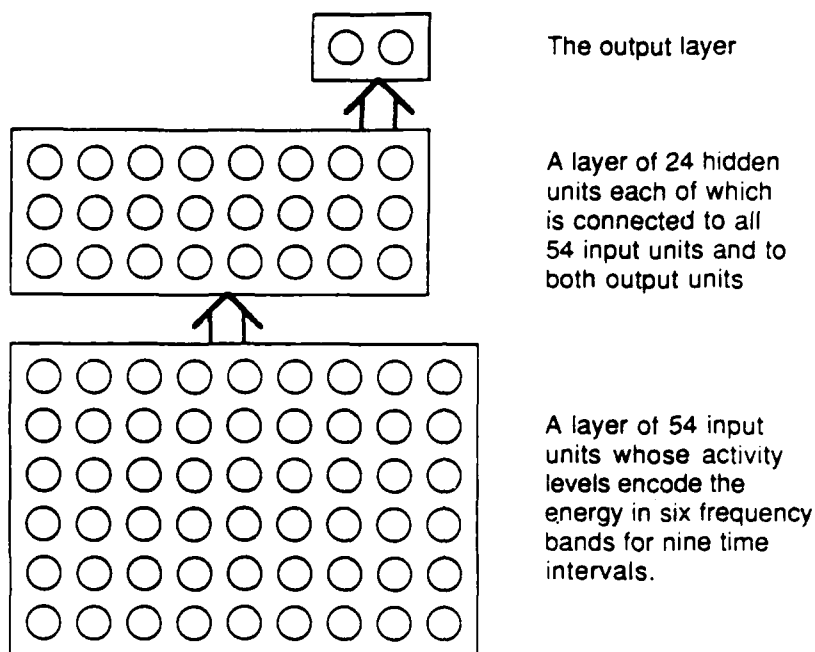


Figure 2-3: The net used for discriminating patterns like those in figure 2-2.

very steep and the weights tend to overshoot. Once the weights have settled down, they are near the bottom of a ravine in weight space, and high values of α are required to speed progress along the ravine and to damp out oscillations across the ravine. We discuss the validity of interpreting characteristics of weight space in terms of structures such as ravines in Section 3.

In addition to the weight changes defined by Eq. 7, we also incremented each weight by $-hw$ each time it was changed, where h is a coefficient that was set at 0.001% for this simulation. This gives the weights a tendency to decay towards zero, eliminating weights that are not doing any useful work. The $-hw$ term ensures that weights for which $\frac{\partial E}{\partial w}$ is near zero will keep shrinking in magnitude. Indeed, at equilibrium the magnitude of a weight will be proportional to $\frac{\partial E}{\partial w}$ and so it will indicate how important the weight is for performing the task correctly. This makes it much easier to understand the feature detectors produced by the learning. One way to view the term hw is as the derivative of $\frac{1}{2}hw^2$, so we can view the learning procedure as a compromise between minimizing E and minimizing the sum of the squares of the weights.

Figure 2-4 shows the activity levels of the units in all three layers for a number of examples chosen at random after the network has learned. Notice that the network is normally confident about whether the example is a riser or a non-riser, but that in difficult cases it tends to hedge its bets. This would provide more useful information to a higher level process than a simple forced choice. Notice also that for each example, most of the units in the middle layer are firmly off.

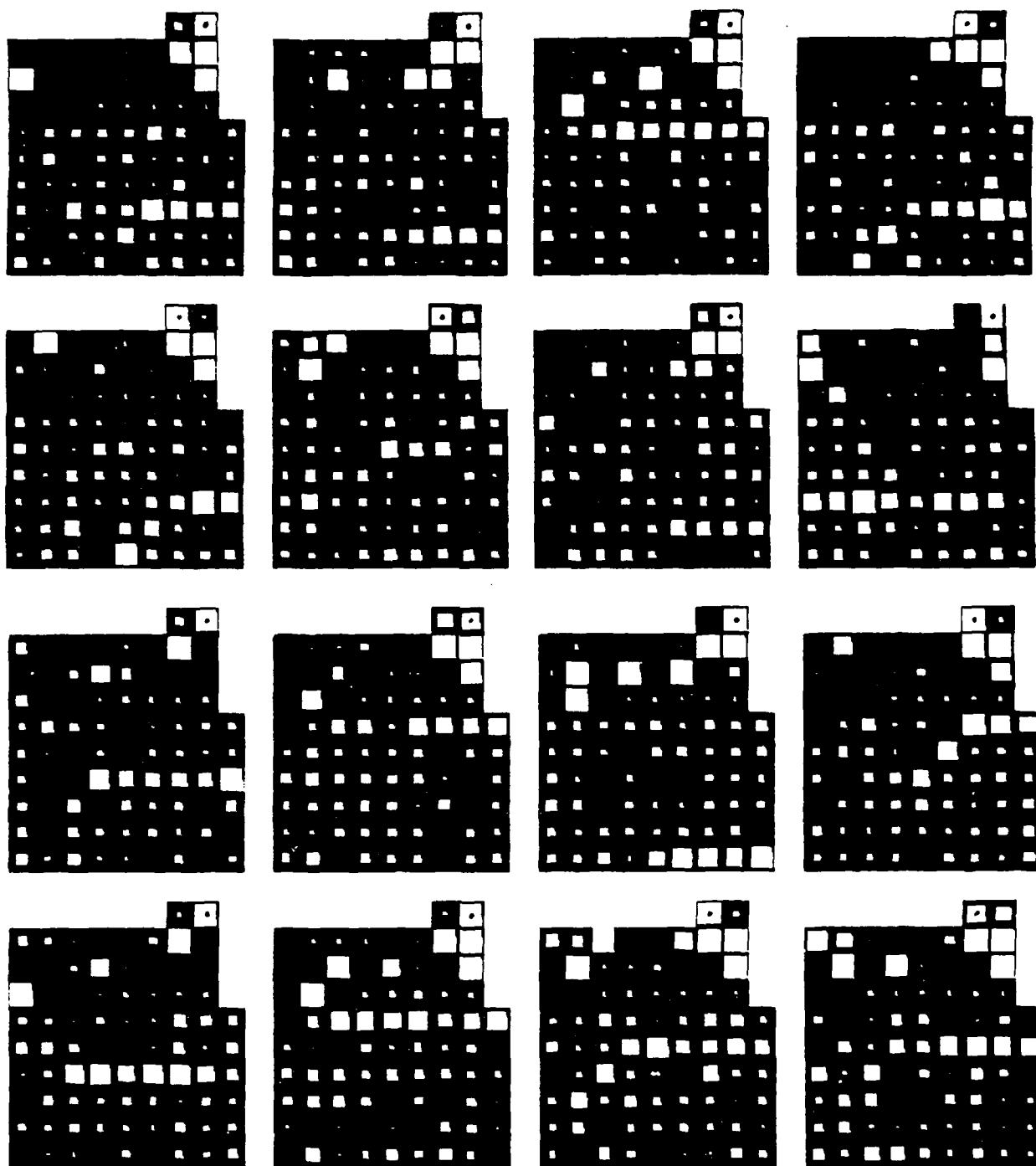


Figure 2-4: Activity levels of units in all three layers for a number of cases.

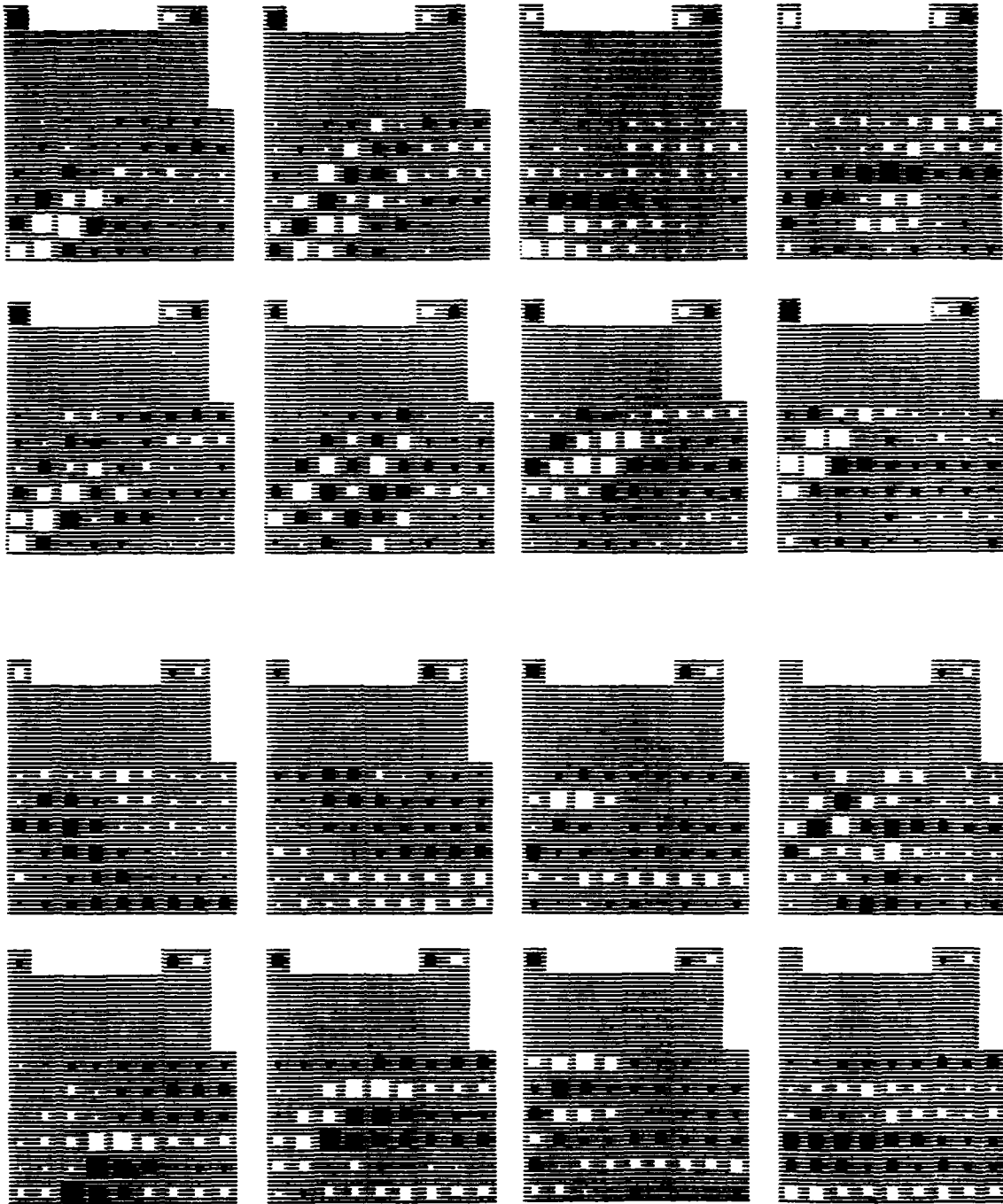


Figure 2-5: Some of the filters learned by the middle layer. Each weight is represented by a square whose size is proportional to the magnitude of the weight and whose color represents the sign of the weight (white for positive, black for negative).

The network was trained for 10,000 blocks of 25 examples each. After this amount of experience the weights are very stable and the performance of the network has ceased to improve. If we force the network to make a discrete decision by interpreting the more active of the two output units as its response, it give the "correct" response 97.8% of the time. This is better than a person can do using elaborate reasoning, and it is probably very close to the optimal possible performance. No system could get 100% correct because the very same data can be generated by adding noise to two different underlying signals, and hence it is not possible to recover the underlying signal from the data with certainty. The best that can be done is to decide which category of signal is most likely to have produced the data and this will sometimes not be the category from which the data was actually derived. For example, with the signal and noise levels used in this example, there is a probability of about 1.2% that the two crucial input units that form the rising part of a riser will have a smaller combined activity level than the two units that would form part of a non-riser with the same onset time and same final frequency. This is only one of several possible errors.

Figure 2-5 shows the filters that were learned in the middle layer. The ones that have positive weights to the "riser" output unit have been arranged at the top of the figure. Their weights are mainly concentrated on the part of the input that contains the critical information, and between them they cover all the possible frequencies and onset times. Notice that each filter covers several different cases and that each case is covered by several different filters. The set of filters form an "ecology" in which each one fills a niche that is left by the others. Using analytical methods it would be very hard to design a set of filters with this property, even if the precise characteristics of the process that generated the signals were explicitly given. The difficulty arises because the definition of a good set of filters is one for which there exists a set of output weights that allows the correct decision to be made as often as possible. The input weights of the filters cannot be designed without considering the output weights, and an individual filter cannot be designed without considering all the other filters. This means that the optimal value of each weight depends on the value of every other weight. The learning procedure can be viewed as a numerical method for solving this analytically intractable design problem. Current analytical investigations of optimal filters [Torre 86] are very helpful in providing understanding of why some filters are the way they are, but they shed little light on how biological systems could arrive at these designs.

3. Characteristics of Weight Space

As mentioned in the Introduction, a useful way to interpret the operation of the learning procedure is in terms of movement down an error surface in multi-dimensional *weight space*. For a network with only two connections, the characteristics of the error surface for a particular task are relatively easy to imagine by analogy with actual surfaces which curve through three-dimensional physical space. The error surface can be described as being comprised of hills, valleys, ravines, ridges, plateaus, saddle points, etc. In the learning procedure, the effects of the weight-change step (ϵ) and momentum (α) parameters have natural interpretations in terms of physical movement among such formations. Unfortunately, for more useful networks with hundreds or thousands of connections it is not clear that these simple intuitions about the characteristics of weight space are valid guides to determining the parameters of the learning procedure.

One way to depict some of the structure of a high-dimensional weight space is to plot the error curves (i.e.

cross-sections of the error surface) along significant directions in weight space and compare them to error curves along random directions. The collection of curves represents the error surface "collapsed" onto two dimensions. While such a graph gives a far from complete picture of weight space, it may give us a more direct way to test the effects of different learning parameters as well as clarify our interpretation of movement in weight space in terms of simple three-dimensional constructs.

As an example, we present a few collapsed error surface graphs of a typical learning problem at various points in the search for a good set of weights. The problem we will consider is learning the association of 20 pairs of random binary vectors of length 10. The procedure will operate on a three-layered network, with 10 input units, 10 hidden units, and 10 output units. Each input unit is connected to each hidden unit, and each hidden unit is connected to each output unit. Taking into account the connections from a permanently active unit to the hidden and output units (used to encode thresholds), the network has a total of 220 connections.

Each curve in a graph is generated by (1) choosing a direction in weight space; (2) changing the connection weights in the network by some factor times the normalized vector representing that direction; and (3) plotting the error produced by the network with the modified connection values. In addition to a number of random directions (dotted curves), two significant directions are shown (solid curves): the direction of maximum gradient and the direction of the last weight step (integrated gradient). Each curve is labeled on the right with its angle (in degrees) from the direction of maximum gradient. An asterisk (*) marks the current position in weight space, and a vertical bar (|) marks the next position.

Figures 3-1 to 3-4 show collapsed error surface graphs for the problem above at points throughout the operation of the learning procedure. Graphs are presented for the first 10 epochs, as well as for epochs 25, 50, 75 and 107 (when a solution is reached).² For the example, $\epsilon=0.1$ and initially $\alpha=0.5$.

During the first few epochs, the procedure repeatedly reaches a minimum along the current weight-change direction and must use the influence of the maximum gradient to change directions. Since momentum contributes to maintaining movement along a particular direction, it is important in these early stages that momentum be low, so as not to dominate the new gradient information. The effect of having momentum too high at the start of learning will be illustrated in later graphs. It is not until epoch 9 or 10 (figure 3-3) that continued movement along the last weight-change direction would be beneficial.

By epoch 25, the directions of maximum gradient and integrated gradient are practically identical and monotonically decreasing over a relatively long distance in weight space. In contrast, the error curve in each of the random directions slopes upwards almost immediately as we move away from the current point. The intuitive interpretation is that the learning procedure is moving slowly along the bottom of a *ravine* in weight space. Because of the correspondence of the directions of maximum gradient and integrated gradient, increasing momentum would speed up movement through the ravine without causing divergent oscillations onto the walls of the ravine. Accordingly, momentum (α) was increased to 0.95 at this point.

²The reader should note that in the graphs the error range changes from [10,50] to [0,40] between epochs 10 and 25.

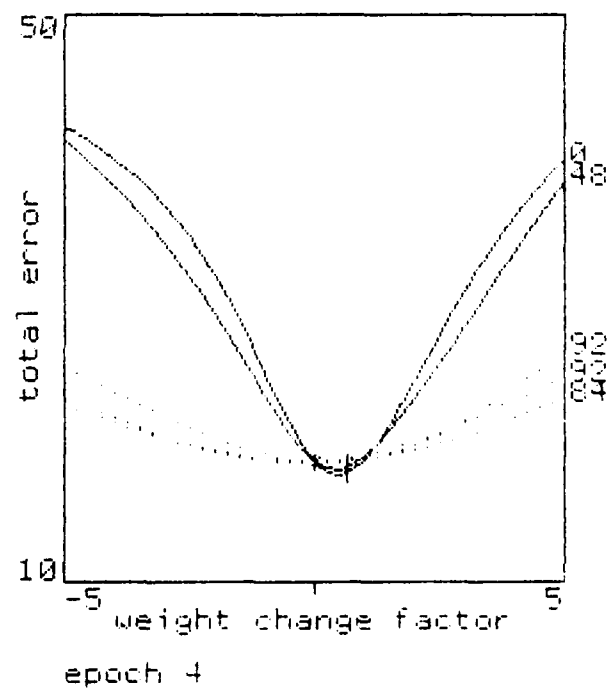
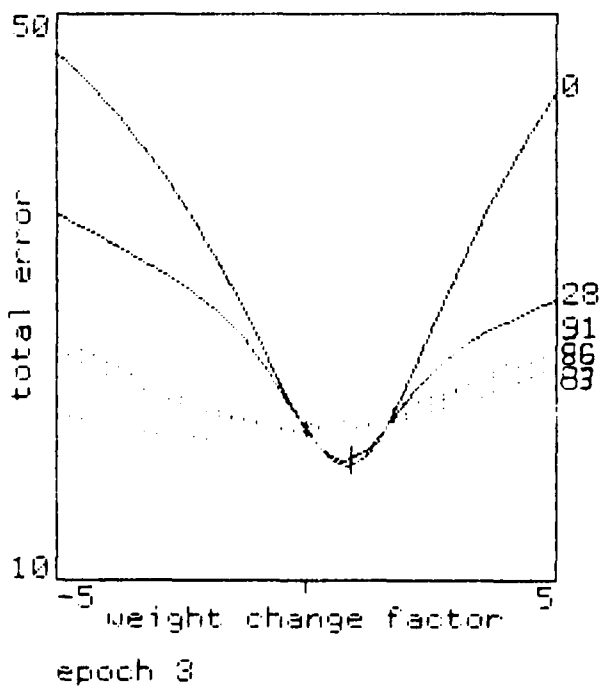
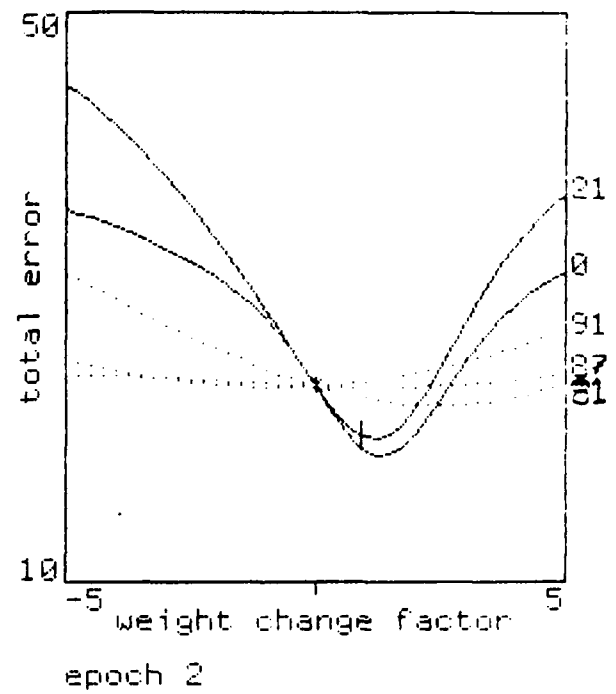
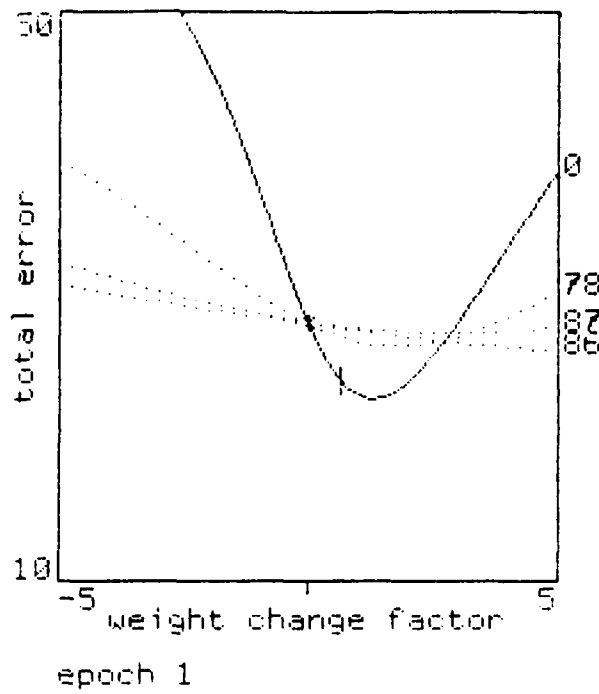


Figure 3-1: Collapsed error surfaces for epochs 1 to 4.

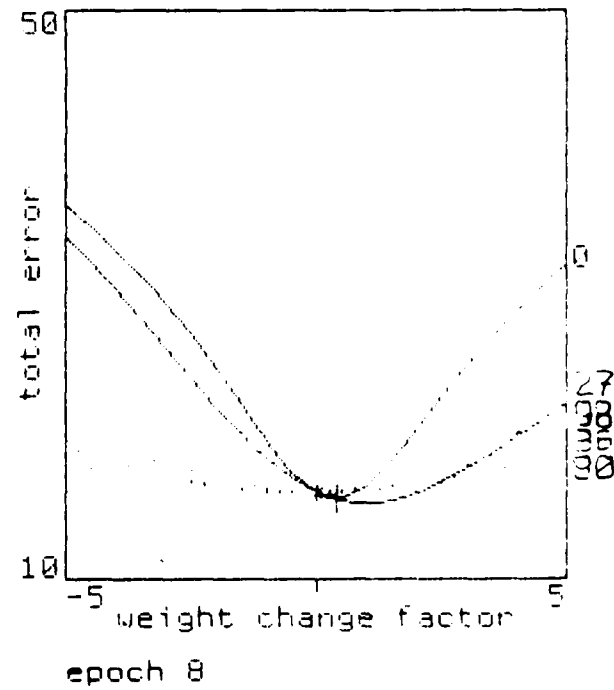
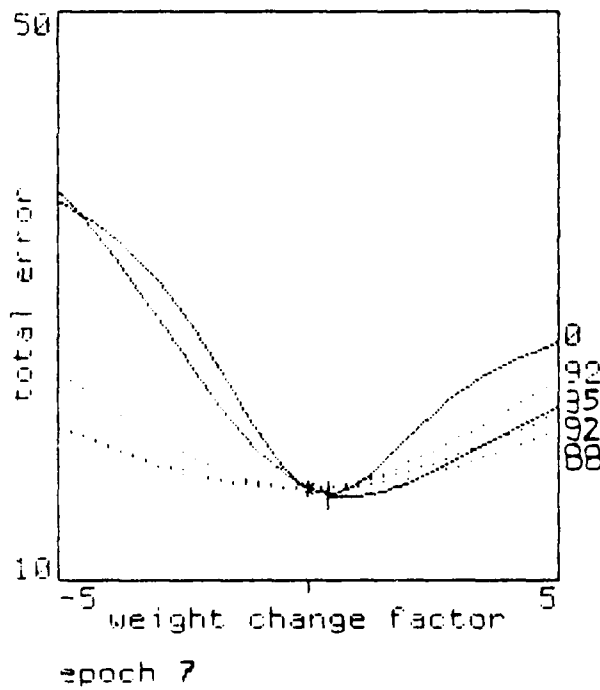
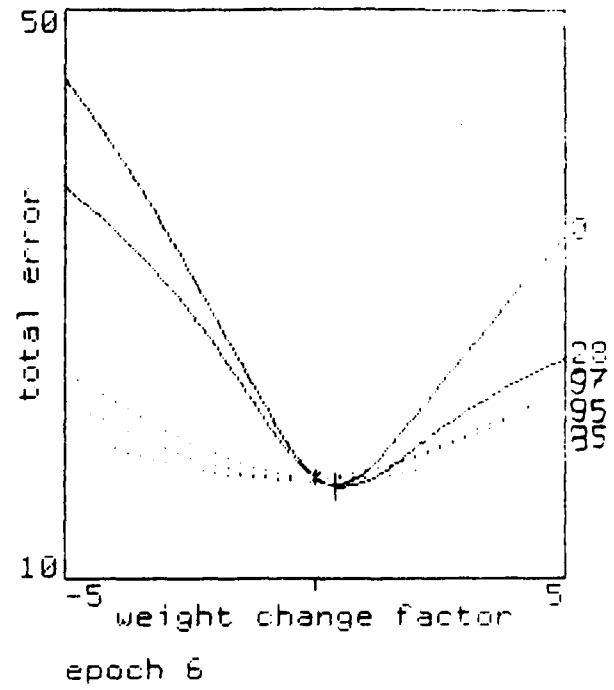
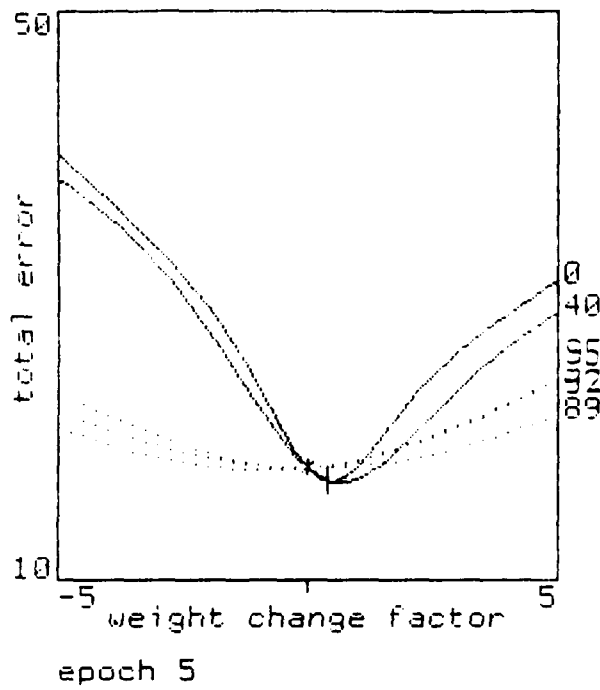


Figure 3-2: Collapsed error surfaces for epochs 5 to 8.

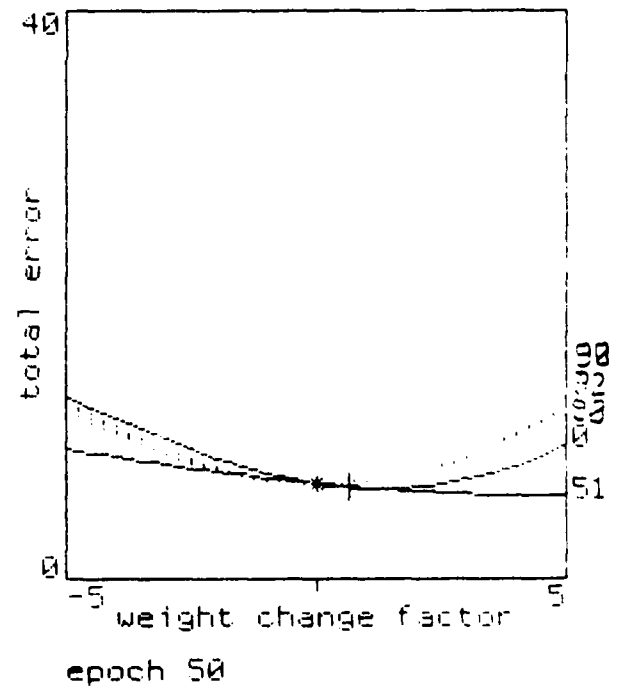
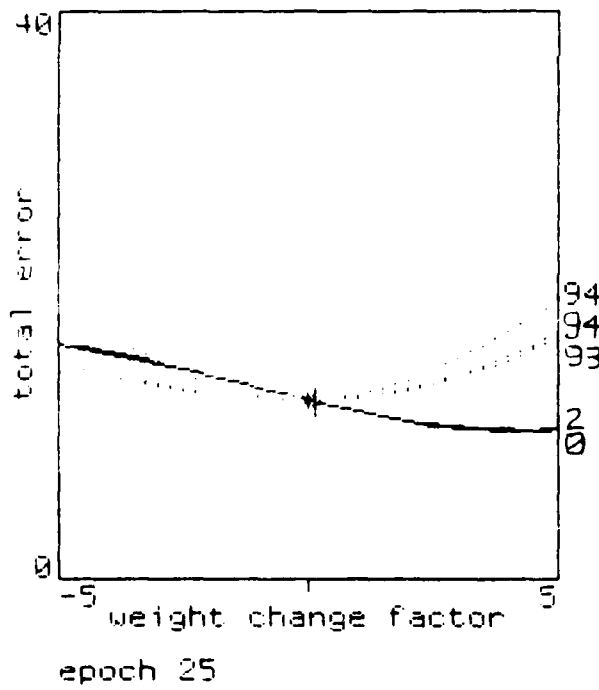
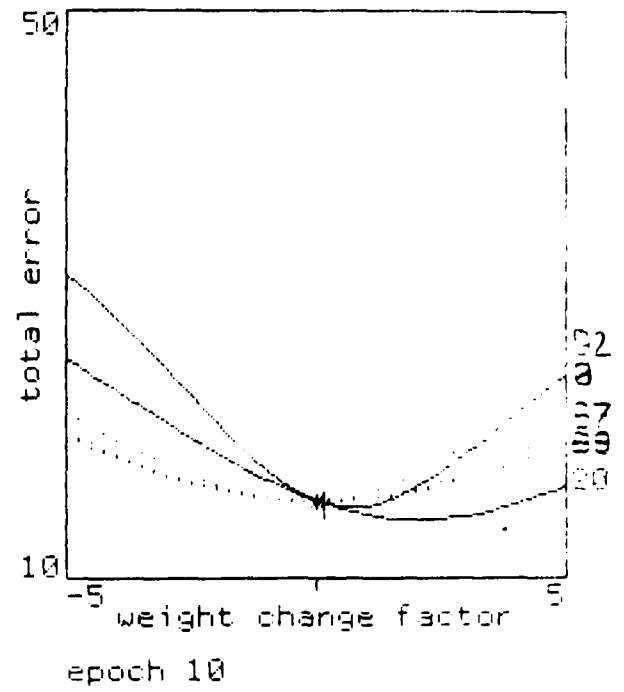
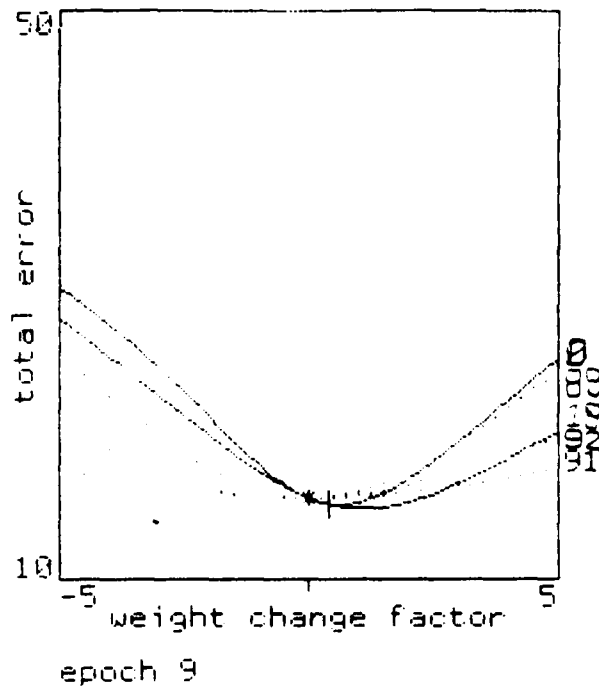


Figure 3-3: Collapsed error surfaces for epochs 9 to 50

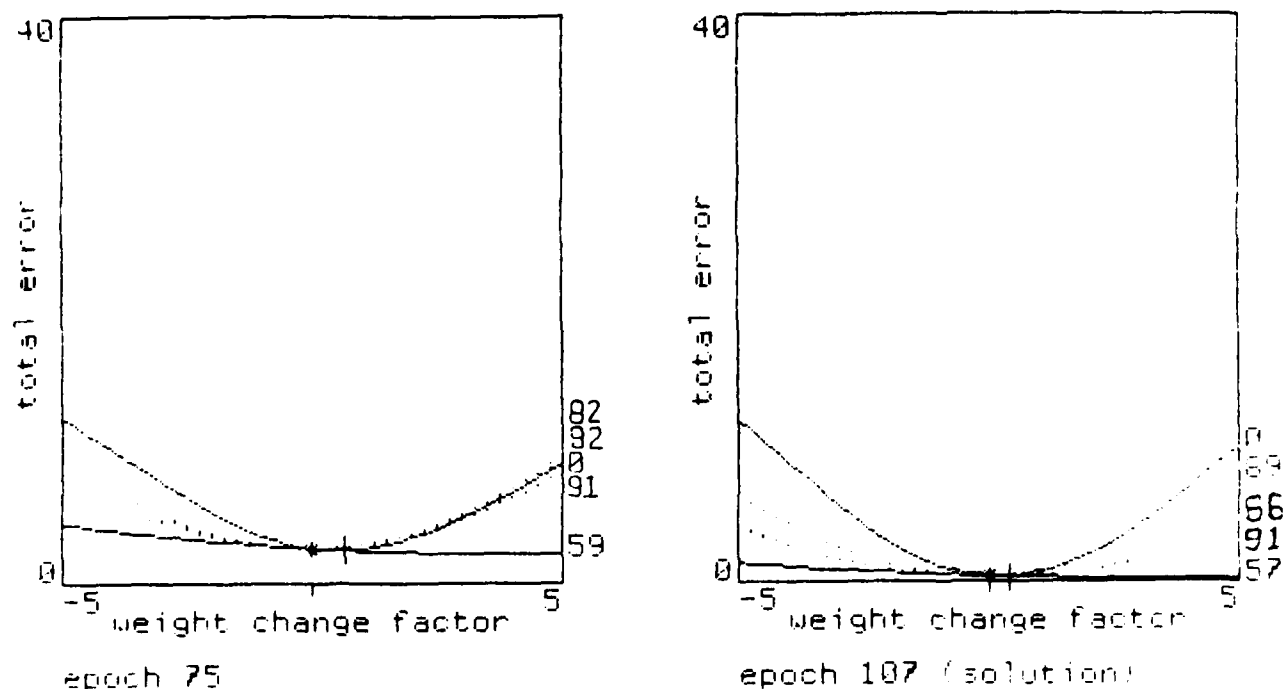


Figure 3-4: Collapsed error surfaces for epochs 75 and 107 (solution)

While the integrated gradient (and hence the direction of weight change) is still pointed along the bottom of the ravine at epoch 50, the direction of maximum gradient now points somewhat across the ravine. Without momentum, the learning procedure would "slosh" from side to side along the walls of the ravine. The high momentum both dampens this oscillatory contribution and maintains movement along the most effective direction. This effect of momentum becomes increasingly important during the later stages of learning, as is evident at epoch 75 (figure 3-4), and finally at epoch 107, when a solution is reached.

These graphs suggest that momentum should be set initially rather low, and only raised when the learning procedure has settled on a stable direction of movement. In order to illustrate the behavior of the procedure when this rule is violated, figure 3-5 presents the collapsed error surface graphs of the first four epochs of a run with momentum set initially to 0.9 (instead of 0.5). The first epoch is fine, since there is no integrated gradient to affect the weight change. However, by epoch 3 the overly high momentum has caused the procedure to overshoot the minimum of the original weight-change direction and *increase* the total error over the last position in weight space.

In the first example run, almost 50 epochs were required to reduce the total error from just over 5.0 to the solution criterion (near 0.0), even with very high momentum (0.95). This suggests the possibility of increasing the size of each weight step to speed up the later stages of learning when high momentum has essentially fixed the direction of

weight change. In fact, increasing ϵ does significantly reduce the number of epochs to solution, as long as the weight step is not so large that the procedure drastically changes direction. However, because a number of changes of direction are required in the early stages of learning, the weight step must not be too large initially. Figure 3-6 illustrates the divergent behavior that results at the beginning of a run with ϵ set to 0.5 (instead of 0.1). The first step drastically overshoots the minimum along the direction of maximum gradient. Successive steps, though smaller, are still too large to produce coherent movement.

4. How the Learning Time Scales

Small-scale simulations can only provide insight into the behavior of the learning procedure in larger networks if there is information about how the learning time scales. Procedures that are very fast for small examples but scale exponentially are of little interest if the goal is to understand learning in networks with thousands or millions of units. There are many different variables that can be scaled:

1. The number of units used for the input and output vectors and the fraction of them that are active in any one case.
2. The number of hidden layers.
3. The number of units in each hidden layer.
4. The fan-in and fan-out of the hidden units.
5. The number of different input-output pairs that must be learned, or the complexity of the mapping from input to output.

Much research remains to be done on the effects of most of these variables. This section only addresses the question of what happens to the learning time when the number of hidden units or layers is increased but the task and the input-output encoding remain constant. If there is a fixed number of layers, we would like the learning to go faster if the network has more hidden units per layer.

4.1. Experiments

Unfortunately, two initial experiments showed that increasing the number of hidden units or hidden layers slowed down the learning.³ In the first, two networks were compared on the identical task: learning the associations of 20 pairs of random binary vectors of length 10. Each network consisted of three layers, with 10 input units and 10 output units. The first (called a 10-10-10 network) had 10 hidden units receiving input from all 10 input units and projecting to all 10 output units; the second (called a 10-100-10 network) had 100 hidden units fully interconnected to both input and output units. Twenty runs of each network on the task were carried out, with $\epsilon=0.1$ and $\alpha=0.8$.

The results of this first experiment made it clear that the learning procedure in its current form does not scale well with the addition of hidden units: the 10-10-10 network took an average of 212 epochs to reach solution, while the 10-100-10 network took an average of 531 epochs.⁴

³We measure learning time by the number of sweeps through the set of cases that are required to reach criterion. So the extra time required to simulate a larger network on a serial machine is not counted.

⁴The reader will note that the example run presented in Section 3 on the apparently identical task as described here took a network with 10 hidden units only 107 epochs to solve. The difference is due to the use of a different set of 20 random binary vector pairs in the task.

The second experiment involved adding additional layers of hidden units to a network and seeing how the different networks compared on the same task. The task was similar to the one above, but only 10 pairs of vectors were used. Each network had 10 input units fully interconnected to units in the first hidden layer. Each hidden layer had 10 units and was fully interconnected to the following one, with the last connected to the 10 output units. Networks with one, two and four layers of hidden units were used. Twenty runs of each network were carried out, with $\epsilon=0.1$ and $\alpha=0.8$.

The results of the second experiment were consistent with those of the first: the network with a single hidden layer solved the task in an average of 100 epochs; with two hidden layers it took 160 epochs on average, and with four hidden layers it took an average of 373 epochs to solve the task.

4.2. Unit Splitting

There is one method of introducing more hidden units which has no effect on the performance of the network. Each hidden unit in the old network is replaced by n identical hidden units in the new network. The input weights of the new units are exactly the same as for the old unit, so the activity level of each new unit is exactly the same as for the old one in all circumstances. The output weights of the new units are each $\frac{1}{n}$ of the output weights of the old unit, and so their combined effect on any other unit is exactly the same as the effect of the single old unit. Figure 4-1 illustrates this invariant unit-splitting operation. To ensure that the old and new networks remain equivalent even after learning, it is necessary for the outgoing weights of the new units to change by $\frac{1}{n}$ times as much as the outgoing weights of the old unit. So we must use a different value of ϵ for the incoming and outgoing weights, and the ϵ for a connection emanating from a hidden unit must be inversely proportional to the fan-in of the unit receiving the connection.

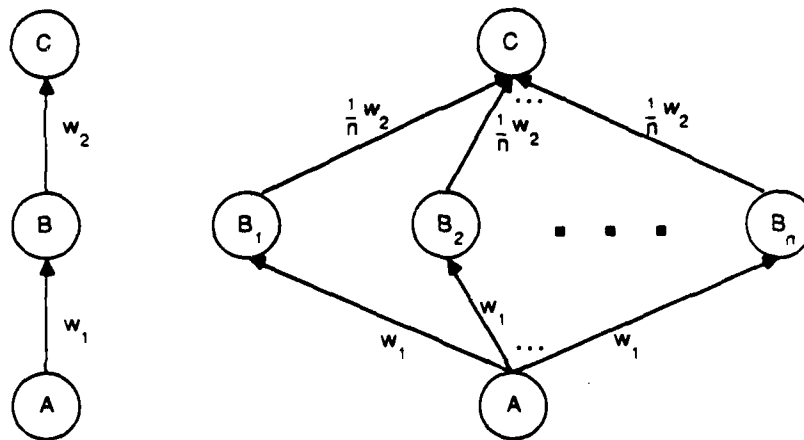


Figure 4-1: These two networks have identical input-output functions. The input-output behavior is invariant under the operation of splitting intermediate nodes, provided the outgoing weights are also decreased by the same factor.

4.3. Varying Epsilon with Fan-In

The fact that it is possible to increase the number of hidden units and connections in a network by a factor of n without affecting the performance of the learning procedure suggests a way to improve how well it scales. Critical to the success of the unit-splitting process is dividing the weight change step (ϵ) by n for weights on replicated connections. This ensures that the weight changes on incoming connections to a unit will cause the same change in total input for a given amount of error produced by the unit, even though n times as many connections are contributing to the input change. The equivalent procedure in a normal network would be to set the effective weight step for a connection, ϵ_{ji} , to be inversely proportional to the fan-in of the unit receiving input via that connection. Presumably such a modification would also improve the scaling of the learning procedure for networks with non-uniform fan-in.

Empirical observations of the operation of the procedure on different sized nets make it clear that larger networks (with higher fan-ins) require a much smaller value of ϵ for optimal learning than do smaller networks. If the change in input to a unit is too large, due to an overly ambitious value of ϵ , the output of the unit may overshoot its optimal value, requiring an input change in the opposite direction during the next epoch. Thus, given the fan-in of units in a network, setting ϵ too high results in oscillatory behavior and poor learning performance. However, if the effective ϵ is reduced for connections leading into units with many inputs but not reduced for other connections, this oscillatory behavior can be avoided without slowing down the learning of weights on connections providing input to units with lower fan-in.

A close look at the details of the backward pass of the learning procedure makes it clear why such a modification would be beneficial. Each connection weight w_{ji} is changed in proportion to the error attributed to the output of unit j , independent of other inputs unit j may receive.

$$\Delta w_{ji} = \epsilon \frac{\partial E}{\partial y_j} y_j (1 - y_j) y_i.$$

Hence, the resulting change in total input to unit j ,

$$\Delta x_j = \sum_{i=1}^n \Delta(w_{ji} y_i)$$

is proportional to n , the fan-in of unit j .

In order to determine if varying ϵ with fan-in would improve the scaling performance of the learning procedure, the scaling experiment involving the addition of hidden units to a single hidden layer was repeated using values of ϵ_{ji} inversely proportional to the fan-in of unit j . The constant of proportionality was set at 1.0 so that the 10-100-10 network had an effective ϵ on the input connections to the output units of 0.01, while the effective ϵ on the input connections to the hidden units remained at 0.1. We expected these more conservative weight change steps to prevent any oscillatory behavior and improve the learning performance.

The results bore out our expectations. The average number of epochs to solution for the 10-100-10 network was reduced from 531 to 121. By varying ϵ with fan-in, the addition of hidden units *speeded up* the learning by almost a factor of two, rather than slowing it down (recall that the 10-10-10 network took 212 epochs on this task). This is

not a solution to the entire scaling problem, but it represents a significant improvement in the ability of the learning procedure to handle large, complex networks.

5. Reducing the Interactions between the Weights

The previous section demonstrated that, by varying ϵ inversely with fan-in, a fully interconnected network with 100 hidden units can learn a task nearly twice as fast as a similar network with only 10 hidden units. While this manipulation of ϵ improves the scaling performance of the learning procedure, many presentations of each environmental case are required to learn most tasks, and larger networks still generally take longer to learn than do smaller ones. The above comparison does not tell us what particular characteristics of a network most significantly influence its learning speed, because at least two important factors are confounded:

1. The number of hidden units.
2. The fan-in of the output units.

However, the learning speed is not necessarily dependent on the *number* of units and connections in a network. This can be seen by considering a network similar to the 10-100-10 network, but in which the layers are not fully interconnected. In particular, the hidden units are partitioned into groups of 10, with each group receiving input from all input units but only projecting to a single output unit. For convenience, we will call this a 10-10of10-10 network. This structure transforms each 10 to 10 mapping into 10 *independent* 10 to 1 mappings, and so reduces the amount of *interaction* between weights on connections leading into the output layer.

5.1. Experiments

In order to investigate the relative effects on learning speed of the number of hidden units, the fan-in of the output units, and the amount of interaction between the weights, we compared the performances of the 10-10-10, 10-100-10, and 10-10of10-10 networks on the task of learning the association of twenty pairs of random binary vectors of length 10. The results of the comparison are summarized in Table 5-1.⁵

As the table shows, the 10-10of10-10 network solves the task much faster than the 10-10-10 network, although both networks have uniform fan-in and the same number of connections from the hidden layer to the output layer. The 10-10of10-10 network learns more quickly because the states of units in each group of 10 hidden units are constrained only by the desired state of a single output unit, whereas the states of the 10 hidden units in the 10-10-10 network must contribute to the determining the states of all 10 output units. The reduced constraints can be satisfied more quickly.

However, when ϵ is varied so that the effects of fan-in differences are eliminated, the 10-10of10-10 network learns slightly slower than the 10-100-10 network, even though both networks have the same number of hidden units and the 10-100-10 network has a much greater amount of interaction between weights. Thus a reduction in the interaction within a network does not always improve its performance. The advantage of having an additional 90 hidden units, some of which may happen to detect features that are very useful for determining the state of the

⁵Data was averaged over 20 runs with $\epsilon=0.1$ in the fixed ϵ cases, $\epsilon_{ij} = 1.0/\text{fan-in}_j$ in the variable ϵ cases, and $\alpha = 0.8$.

	number of hidden units	fan-in of output units	ave. no. of epochs to solution fixed ϵ	variable ϵ
10-10-10	10	10	212	(212)
10-100-10	100	100	531	121
10-10of10-10	100	10	141	(141)

Table 5-1: Comparison of the performance of the 10-10-10, 10-100-10, and 10-10of10-10 networks on the task of learning twenty random binary associations of length 10. Varying ϵ has no effect on networks with uniform fan-in, and so the average number of epochs to solution for these conditions is placed in parentheses.

output unit, seems to outweigh the difficulty caused by trying to make each of those feature detectors adapt to ten different masters. One might expect such a result for a task involving highly related environmental cases, but it is somewhat more surprising for a task involving random associations, where there is no systematic structure in the environment for the hidden units to encode. It appears that, when the magnitudes of weight changes are made sensitive to the number of sources of error by varying ϵ with fan-in, the learning procedure is able to take advantage of the additional flexibility afforded by an increase in the interactions between the weights.

5.2. Very fast learning with no generalization

We can gain some insight into the effects of adding more hidden units by considering the extreme case in which the number of hidden units is an exponential function of the number of input units. Suppose that we use *binary* threshold units and we fix the biases and the weights coming from the input units in such a way that exactly one hidden unit is active for each input vector. We can now learn any possible mapping between input and output vectors in a single pass. For each input vector there is one active hidden unit, and we need only set the signs of the weights from this hidden unit to the output units. If each hidden unit is called a "memory location" and the signs of its outgoing weights are called its "contents", this is an exact model of a standard random-access memory.

This extreme case is a nice illustration of the trade-off between speed of learning and generalization. It also suggests that if we want fast learning we should increase the number of hidden units and also decrease the proportion of them that are active.

6. Back Propagating Desired States

The standard learning procedure informs a unit j of the correctness of its behavior by back propagating error gradient information, $\frac{\partial E}{\partial y_j}$, that tells the unit to be more or less active in this case. The variation of the learning procedure we develop below will back propagate desired state information that will tell a unit whether it should be *active* or *inactive* in this case.

6.1. General Approach

To illustrate the general approach of the new procedure, consider a single output unit receiving input from a number of hidden units. Suppose the output unit wants to be "on" in this case (i.e. has a desired state of 1) but is receiving insufficient input. Each hidden unit can be assigned a desired state depending on the sign of the weight connecting it to the output unit: "on" if the weight is positive, "off" if it is negative.

Now consider a single hidden unit receiving desired state information from all of the output units to which it is connected. For this environmental case, some output units may want the hidden unit to be "on," others may want it to be "off". In order to integrate this possibly conflicting information, we need a way of weighting the influence of each output unit on the determination of the desired state of the hidden unit. Certainly the weight on the connection should be a factor, since it scales the amount of influence the hidden unit has on the state of the output unit. In addition, we will assign a *criticality* factor to the desired state of each output unit, in the range $[0,1]$, that will represent how important it is (to the performance of the network) that the unit be in its desired state. The assignment of these factors to each output unit for each case becomes part of the task specification.

In order to back propagate desired state information, we must calculate the desired state and criticality factor of a hidden unit based on the actual state, desired state and criticality of each output unit to which it is connected. The desired state of the hidden unit will be 1 if the weighted majority of output units want it to be "on" (as described above), and 0 otherwise. If most of the output units agree, then the criticality of the hidden unit should be high, whereas if an approximately equal number of output units want it "off" as want it "on," the criticality should be set low. In general, the criticality of a hidden unit will be a measure of the consistency of the desired state information, calculated according to the formula below.

Each hidden unit in the penultimate layer of the network now has an actual state, desired state, and criticality assigned to it. This allows the desired states and criticalities of the preceding layer to be calculated, and so on until the input units are reached (similar to back propagating error gradient information). All that is left to do is determine the change for each connection weight w_{ji} . The unit j receiving input via the connection has an actual state, desired state and criticality assigned to it. The difference between the desired state and actual state constitutes an error term (identical to the error term of output units in the standard procedure) which, when weighted by criticality and the output of unit i , determines how w_{ji} should be changed to reduce this difference. When the difference between the actual and desired states is minimized for all units in the network (the output units in particular), the network will have learned the task.

A procedure similar to the one described above has been developed by Le Cun [Le Cun 85, Le Cun 86], but with at least two significant differences. The units in Le Cun's networks are binary threshold units, rather than units with real values in the range $[0,1]$. Also, his learning procedure makes no use of an equivalent to our criticality factors. We believe that the combination of these two differences gives our procedure additional flexibility and contributes to its success at avoiding local minima during learning, but only empirical testing will determine which approach is best.

6.2. Details

The details of the forward pass in this variation of the learning procedure are the same as in the standard procedure. The environment clamps the states of the input units, as well as setting the desired states and criticalities of the output units. After the completion of the forward pass, each output unit j has a desired state, d_j , an actual state, y_j , and a criticality, c_j . The desired state of each hidden unit i in the penultimate layer of the network is given by

$$d_i = \text{if } \sum_j w_{ji}(2d_j-1)c_j > 0 \text{ then } 1 \text{ else } 0.$$

The sign of the factor $w_{ji}(2d_j-1)$ determines the direction of influence and the factor c_j determines amount of influence on unit i . The criticality factor for unit i is given by

$$c_i = \frac{|\sum_j w_{ji}(2d_j-1)c_j|}{\sum_j |w_{ji}(2d_j-1)c_j|}$$

so that c_i equals 1 if all of the desired state influences are of the same sign, and 0 if they exactly cancel out (i.e. their sum equals zero). In general, the value of c_i is proportional to the extent to which the desired state influences agree.

Each hidden unit in the penultimate layer now has a desired state, actual state, and criticality assigned to it, so desired state information can be back propagated further through the net until each unit receiving a connection has values assigned to it. At this point we can calculate the appropriate change to each weight Δw_{ji} in the network,

$$\Delta w_{ji}(t) = \epsilon(d_j - y_j)c_j y_i + \alpha \Delta w_{ji}(t-1).$$

The weight changes for each environmental case are summed and carried out at the end of each epoch. The process repeats until the sum of the squared difference between the actual and desired states of the output units falls below a solution criterion.

6.3. General Performance

The above set of equations defines a variation of the standard learning procedure based on desired states rather than error gradients. The amount of interaction between weights in the network is less than in the standard procedure because the error term of a hidden unit is a simple difference between actual and desired states, rather than a weighted sum of the error terms of each unit to which it is connected. Because of this reduced interaction, problems requiring very fine coordination between hidden units may be more difficult (and hence slower) to solve. Our hope is that the procedure will scale better, and hence speed up learning overall for large, loosely constrained tasks.

In order to ensure that the procedure actually worked, it was tested on a standard problem (the 4-2-4 encoder described in Section 7) and various random association tasks. The standard procedure solves the 4-2-4 encoder problem in an average of 108 epochs.⁶ The new procedure was actually slightly faster, taking an average of 95

⁶For twenty runs, with $\epsilon_\mu = 1.0/\text{fan-in}_j$ and $\alpha=0.8$

epochs when it solved the task. Unfortunately, it would fail to solve the task occasionally, settling into a state in which both hidden units essentially represented the same subportion of the task. This is an example in which the reduced interaction prevented the network from solving a task requiring a particular relationship between the hidden units.

On tasks involving learning random binary associations of length 10, the new procedure solved the task every time, but was significantly slower than the standard procedure. Each procedure was run on a fully interconnected network with 10 input units, 10 hidden units, and 10 output units. On a task with 10 association pairs, the new procedure took an average of 219 epoch, compared with 100 epochs for the standard procedure.

Once the viability of the new procedure was established, we tested it on a task that the standard one cannot solve—what might be called the 1-10x1-1 encoder problem. The network has a single input unit, a single output unit, and ten hidden layers, each containing a single unit that is connected to the units in the adjacent layers. The task is for the output unit to duplicate the state of the input unit. The standard procedure fails on this task because the error gradient is greatly reduced as it is back propagated, so that the weights in the lower layers receive negligible information on how to change. In contrast, desired state information does not become weaker as it is passed back through the network, and so the new procedure should be able to solve the task. In fact, it took an average of only 115 epochs to solve.⁷

6.4. Scaling Performance

Since our original motivation for formulating this variation of the learning procedure was to develop a learning procedure that scaled well, we compared the two procedures on how well they scaled with the addition of hidden units to a single layer, and with the addition of hidden layers. Figure 6-1a shows results for three-layered networks with either 10 or 100 hidden units on the task of 10 random binary associations of length 10. While the new procedure takes more epochs to solve the task in general, its performance improves to a greater extent with the addition of hidden units than does the standard procedure. With larger, similarly structured tasks, the new procedure might indeed perform better.

However, the addition of hidden *layers* impairs the performance of the new procedure significantly more than the standard procedure (see figure 6-1b). This is somewhat surprising, given the success of the new procedure on the 1-10x1-1 encoder problem. Its occasional failure on the 4-2-4 encoder problem suggests a reason for its poor scaling behavior with multilayered networks. The pressure for hidden units in a layer to differentiate function is reduced in the new procedure as a result of the reduced interaction between the units. As the number of layers in a network is increased, information from the output units exerts less differentiating influence on early layers. As a result, hidden units in early layers become overly redundant at the expense of being able to encode some information necessary to solve other aspects of the task. It seems that this over-redundancy is difficult to unlearn and slows the solution of the task when using a multilayered network. An additional pressure on the hidden units in a layer to take on separate functions (perhaps some sort of decorrelation, or lateral inhibition) would have to be added to the

⁷With a very large value of ϵ , for example 10.0, the new procedure takes only 32 epochs on average to solve the 1-10x1-1 encoder problem.

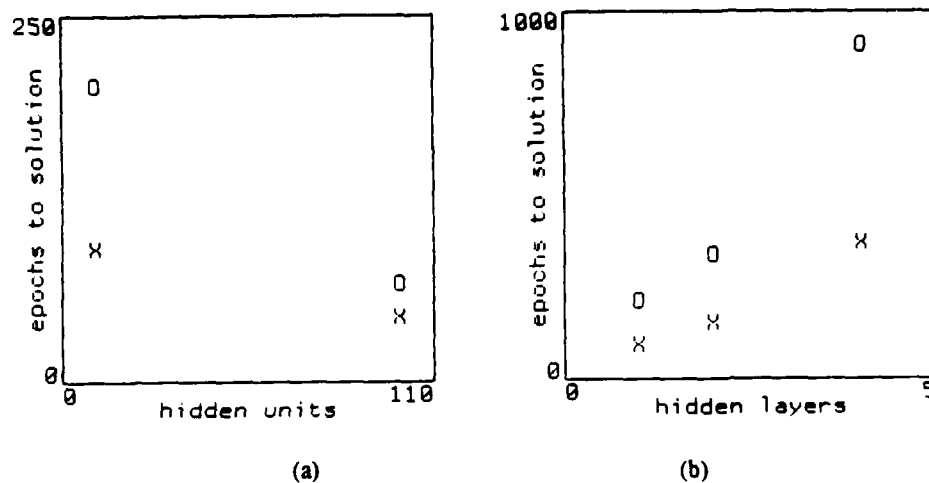


Figure 6-1: Comparison of the effect of adding (a) hidden units, or (b) hidden layers, on the speed of learning by back propagating error gradients (X) or desired states (O).

procedure to make it feasible to use with large networks in which the input and output units are separated by a significant number of hidden layers.

6.5. Conclusions on Back Propagating Desired States

While back propagating desired states appears to scale well under certain circumstances, it is slow to solve (and occasionally fails at) problems that require precise or extensive coordination among the hidden units in a layer. The lack of interaction causes over-redundancy that prevents the procedure from solving certain tasks. The addition of a separate mechanism to reduce this redundancy may improve its performance on highly constrained tasks like the 4-2-4 encoder, but would most likely reintroduce the interactions that the method was designed to eliminate and impair its ability to scale well with an increase in network size.

The amount of interaction present in a learning procedure seems to determine a tradeoff between being able to solve small, highly constrained tasks quickly and being able to solve large, less constrained tasks quickly. Perhaps it is a mistake to expect an procedure to do both well, and we should design our learning procedures and networks with more careful consideration of the tasks they are to solve.

7. Gain Variation in Iterative Nets

7.1. Introduction

The extension of the learning procedure to iterative networks was described in Section 1. Until now, we have only considered the behavior of networks on a relatively large time scale, within which gradual weight changes can be interpreted as movement with respect to an error measure in weight space. Iterative networks have interesting behavior on a smaller time scale as well, analogous to movement in *state space*. During each input-output

presentation the global state of the network varies as the units in the network interact with each other to reach some final (possibly stable) global state. Since we will mainly be concerned with iterative nets that settle into a stable or nearly stable state, we will refer to the shorter time scale as a *settling*. The results developed so far for the learning procedure have concentrated on effects over the larger time scale. It is also possible to investigate the variation of parameters over the smaller time scale. One such parameter that may be varied as the network settles is the amount of *gain* at the inputs of individual units. Motivation for such study may be found in work which has investigated gain effects in other types of networks.

The continuous valued units used in the back propagation networks can be related to the stochastic units used in Boltzmann Machines [Hinton 83, Ackley 85]. The sigmoid function used to determine the output value of the continuous unit is the same function used to determine the probability distribution of the state of a binary-valued Boltzmann unit. The output of the continuous unit can be interpreted as representing the expected value of an ensemble of Boltzmann units, or equivalently, the time average of a single unit, if no other units change state. This relationship between the probability distribution of the state of a unit in a Boltzmann Machine and the value of the output of a continuous unit in a back propagation net allows one to relate gain variation to simulated annealing [Kirkpatrick 83]. In a Boltzmann Machine the probability of a unit having output 1 is

$$p_k = \frac{1}{1 + e^{-\Delta E_k/T}}$$

where T is the annealing temperature, and the energy term is simply a weighted sum of the inputs to a unit. In a back propagation net with variable gain the output of a unit is

$$y_j = \frac{1}{1 + e^{-G \sum_i w_{ji} x_i}}$$

where G is the gain term.

It has been shown that simulated annealing is a good method to improve the ability of networks of stochastic units to settle on a globally optimal solution [Kirkpatrick 83, Ackley 85]. Since gain in iterative networks plays a role analogous to the inverse of temperature in Boltzmann Machines, allowing the system to vary the gain as it settles may also improve the convergence of iterative networks.

Stronger support for gain variation in iterative nets comes from recent work by Hopfield and Tank [Hopfield 85]. The authors examined the ability of networks of non-linear analog units to settle into a better than random solution to the Traveling-Salesman Problem. The units in their network are modelled by analog rather than digital components, producing an input-output relation that is a continuous function of time. However, the input-output relation is defined by a sigmoid applied deterministically to the weighted sum of the inputs. Thus each unit in a Hopfield and Tank net is very similar to a unit in a back propagation net.

Hopfield and Tank show that the solution reached by their networks with a fixed gain u_0 is equivalent to the effective field solution of a thermodynamic equilibrium problem with an effective temperature $kT = u_0/2\tau$, where T is temperature, k is a proportionality constant, and τ is a parameter representing the time over which the input is

integrated. Furthermore, the effective field solution when followed from high temperatures will lead to a state near the thermodynamic ground state (i.e. a state near the global energy minimum of the system). The authors note that

A computation analogous to following effective field solutions from high temperatures can be performed by slowly turning up the analog gain from an initially low value [Hopfield 85, p. 150].

[Hopfield 85] provides some insight into why it is helpful to start with low gain. If the outputs of the units are confined to the range $[0,1]$ then the possible states of the system are contained within an n -dimensional hypercube, where n is the number of output units. In the high gain limit, the stable states of the network (i.e. minima of the energy function) are located at the corners of the hypercube. With lower gain, the stable states migrate towards the center of the volume defined by the hypercube. As they move inwards, minima that are distinct with higher gain merge. Each minimum of the low gain system represents a whole *set* of similar high gain minima. By starting at low gain it is therefore possible to select a *set* of promising high gain minima, without yet becoming committed to a particular minima within that set. Further search refines this set as the gain is increased.

Hopfield and Tank's results indicate that gain variation, and in particular a slow increase in gain during settling, can improve the performance of iterative nets, but care must be taken in extending these results to cover iterative back propagation nets. The nets investigated by Hopfield and Tank had symmetric connections. For such networks there is a global energy function that determines the behavior of the network, and the stable states of the network are minima of this energy function [Hopfield 82]. No such conditions hold for the general asymmetric nets used by back propagation.⁸ In addition, the Hopfield and Tank nets were allowed to settle until they reached equilibrium, while the typical iterative back propagation net is only allowed to settle for a fixed number of time steps and may not reach equilibrium. Finally, the Hopfield and Tank nets have a fixed set of weights, while the weights of the iterative back propagation net change between settlings.⁹ Although this difference is not directly relevant to the application of gain variation to the networks, it does raise interesting questions about whether improving performance in the state space will affect search in the weight space.

Empirical results also suggest that gain variation may be useful in iterative back propagation nets. In most experiments a problem is considered solved when the global error measure drops below some specified criterion. Further improvements are still possible once this criterion is reached, and often these improvements are obtained by increasing the magnitude of all weights in the network. This is equivalent to raising the gain.

In what follows we present some results of investigations of gain variation in iterative networks using the back propagation procedure. Recall that for every iterative net with a finite number of time steps in which to settle there is an equivalent layered net in which each layer represents a separate time step (see figure 1-2). In a standard iterative net, the input to a unit at each time step is a weighted sum of the outputs of units in the previous time step (or previous layer in the equivalent layered net). The corresponding weights in each layer (i.e. time step) of the network are constrained to be identical.

⁸It is important not to confuse the global energy function that determines the stable states of a network as it settles with the global error function used to guide the search for a good set of network weights.

⁹The set of weights is held constant within the shorter time scale of a settling, but is varied over the longer time scale.

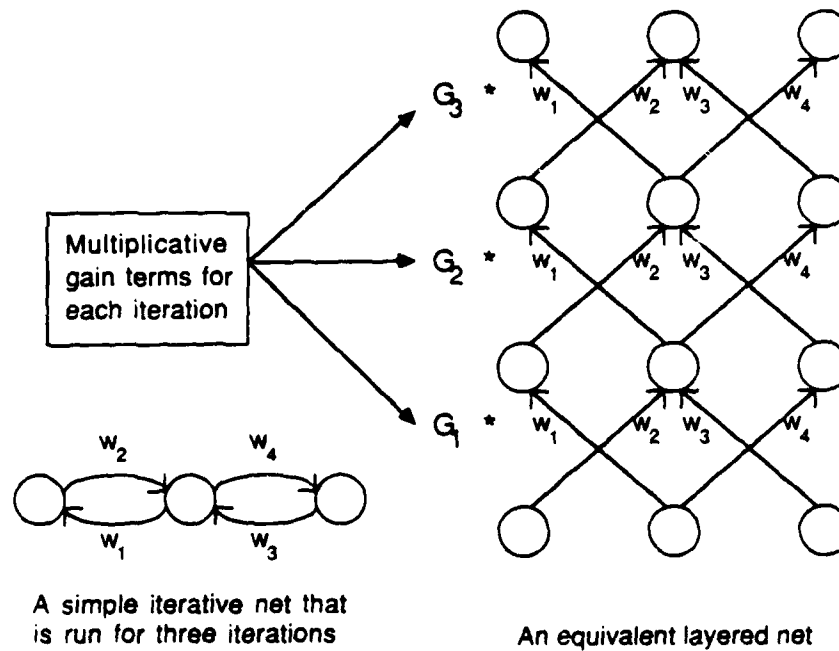


Figure 7-1: An iterative net and the equivalent layered net, with gain variation.

In networks with gain variation this model is extended slightly. The extension is most easily illustrated by reference to the equivalent layered network representation. A multiplicative global gain term is defined for each layer of the net (see figure 7-1). The input to each unit is now a weighted sum of the outputs of units in the previous layer times the global gain term for that layer. The corresponding weights in each layer are identical, as before, but the global gain is allowed to vary across layers. Translating back to the iterative net terminology, the gain is allowed to vary across time steps as the network settles.

7.2. Implementation of Gain Variation

The optimal gain variation in an iterative net is to be "learned" by the system by applying the back-propagation procedure to the gain terms of each time step. This approach is equivalent to performing a gradient descent search for the optimal values of the gain terms in the error measure defined by Eq. 3. In Section 1 we derived the gradient of this error measure with respect to each weight in the network (see Eq. 5).

To extend this development to networks with variable gain it is easiest to consider the gain to be a multiplicative term applied to the input for each unit.

$$x_{j,t} = G_t \sum_i w_{ji} y_{i,t}$$

where G_t represents the global gain at time t , and $x_{j,t}$ is the summed input to unit j . This is the same input as in a

normal iterative net except for the multiplicative gain term (c.f. Eq. 1). The w_{ji} terms are constant for all time steps of the settling, while the G_t term and $y_{i,t}$ terms vary across the settling.

It is possible to derive expressions for the gradient of the error with respect to each w_{ji} and with respect to each G_t . For the w_{ji} terms application of the chain rule yields

$$\frac{\partial E}{\partial w_{ji}} = \sum_t \frac{\partial E}{\partial x_{j,t}} \cdot \frac{\partial x_{j,t}}{\partial w_{ji}}.$$

Evaluating the derivative of the total input with respect to each weight yields

$$\frac{\partial E}{\partial w_{ji}} = \sum_t \frac{\partial E}{\partial x_{j,t}} G_t y_{i,t}.$$

We must sum the contributions to the error gradient from each time step in order to maintain the equivalence of corresponding weights across time steps, as pointed out in Section 1.4.

To determine the gradient of the error with respect to each gain term we must sum the contribution of each unit for that time step.

$$\frac{\partial E}{\partial G_t} = \sum_j \frac{\partial E}{\partial x_{j,t}} \cdot \frac{\partial x_{j,t}}{\partial G_t}.$$

These derivatives must be evaluated separately for each time step in order to determine the optimal gain variation during a settling.

Both $\frac{\partial E}{\partial w}$ and $\frac{\partial E}{\partial G}$ are averaged over all input cases before the values of G_t or w_{ji} are updated. In addition, the w_{ji} gradients are also averaged over iterations, while a separate gradient must be maintained for each time step for the gain terms.

We use the standard acceleration method in modifying each w_{ji} (see Eq. 7), but the gain terms are modified using a strict gradient descent method without the acceleration term.

$$\Delta G_t = -\epsilon_G \frac{\partial E}{\partial G_t}.$$

7.3. Experimental Results

Two results were expected when gain variation was implemented in the iterative nets:

1. Networks would develop a gain schedule in which an initially small gain would be increased monotonically over the settling period.
2. Networks would reach a solution to a problem in fewer iterations of the learning procedure.

The first expectation is based on the work on annealing in stochastic networks and Hopfield and Tank's work. The second expectation is based on the fact that a network using a suitable gain schedule can outperform a network with the identical set of weights but without gain variation. Allowing the network to vary the gain as it settles improves the ability of the network to find a stable state close to the global optimum. This effect can have an

indirect influence on the weight space search since if a better solution can be found for a given weight set, then less fine tuning of the weights will be required to reach the solution criterion. Since the number of stable states (hence possible local optima) increases with network size, these effects should be more noticeable with large networks.

Two different tasks were used to investigate the effects of gain variation. The first task was the 4-1-4 encoder problem, very similar to the 4-2-4 encoder described in [Ackley 85]. The 4-2-4 network has three layers, with 4 units in each of the input and output layers and 2 units in the hidden layer. Each hidden unit is connected to all of the input units and all of the output units. The task of the network is to learn a mapping such that when a single input unit is turned on, the corresponding output unit will be turned on.¹⁰ The 4-1-4 network differs from the 4-2-4 network in that only a single hidden unit is used, and each output unit is connected in both directions with each other output unit (see figure 7-2). This interconnectivity allowed the output units to learn to mutually inhibit each other, thus forming a *winner-take-all* network [Feldman 82]. The network was presented with each input vector and then allowed 5 cycles to settle before the output was examined and an error measure calculated. As with the layered networks, error gradients were averaged over all input cases before updating the weights.

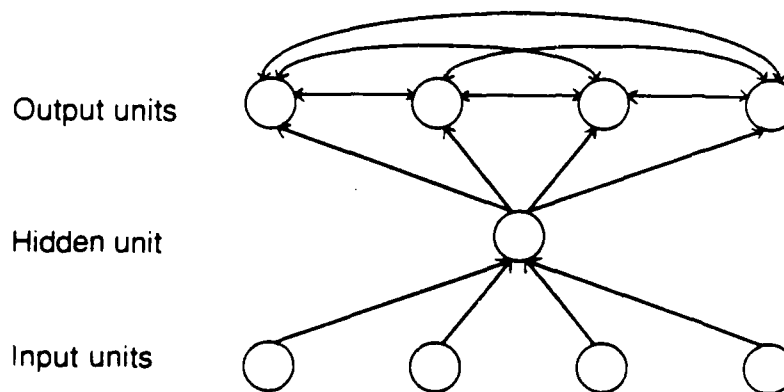


Figure 7-2: The 4-1-4 encoder network.

Twenty sets of runs were performed. In each run the weight step and momentum were held constant ($\epsilon=0.1$, $\alpha=0.9$) while the gain step, ϵ_G , was varied systematically from 0.0 to 0.06 in steps of 0.002. Each run began with a different set of small random weights. The results supported our predictions. Without gain variation the network required an average of 2269 epochs to find a solution; with gain variation the average was reduced to 566 epochs.¹¹ Figure 7-3 presents the number of epochs required to reach solution versus the gain step size for a typical run. Note that the graph tends to decay exponentially. Introducing even a moderate amount of gain variation can yield significant improvements, but the amount of improvement rapidly levels off. Figure 7-4 represents a typical gain

¹⁰The hidden units must use their states to encode which of the 4 input units is on. If units were binary, then the code learned would have to make optimal use of the bandwidth provided by the two hidden units.

¹¹The ranges were 1652 to 3867 epochs without gain variation, 155 to 1000 with gain variation.

schedule learned by the system. The basic shape of the gain schedule was identical in all test runs. As expected the system learns to increase the gain as the system settles. With only five data points it is not possible to fit any particular function to the form of the gain schedule with any great degree of accuracy.

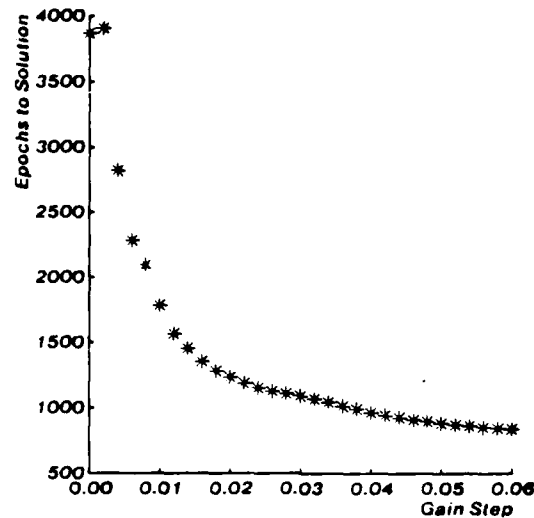


Figure 7-3: Graph of number of epochs to solution vs. gain step size for the 4-1-4 network.

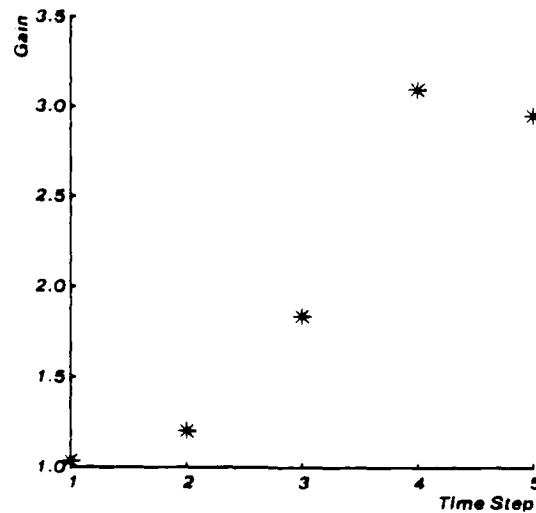


Figure 7-4: Typical gain schedule for the 4-1-4 network.

A second set of test runs was performed on a 10-10-10 network in which the learning task required associating 15 10-bit random vector pairs. In this case both the output and hidden units were fully interconnected (see figure 7-5), and the network was allowed 11 cycles to settle before its output was examined. Ten sample runs were performed in

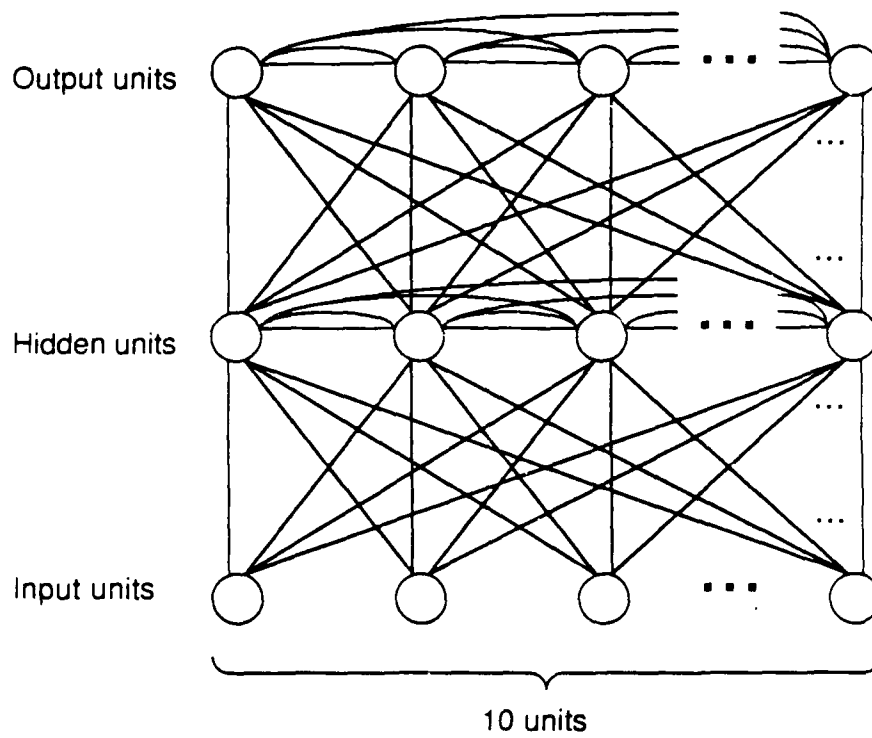


Figure 7-5: The 10-10-10 network used for the association of 10-bit random vector pairs.

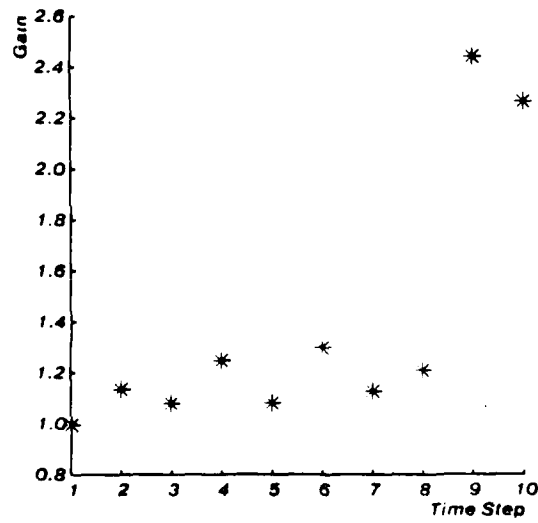


Figure 7-6: Typical gain schedule learned for the 10-10-10 network.

which ϵ and α were held constant ($\epsilon=0.05$, $\alpha=0.8$) and ϵ_G was varied systematically. The results again supported predictions. A typical gain schedule learned by the network is shown in figure 7-6.

In this case the average number of epochs to find a solution was 263 without gain and 184 with gain.¹² The improvement achieved with gain variation in this problem is not as significant as with the 4-1-4 problem, and there was considerable overlap in the values obtained with and without gain. (In two of the sample runs the solution was actually found slightly faster with no gain variation at all.) The reason for this difference may be the greater amount of fine tuning required to find a satisfactory solution for the 4-1-4 nets.

An examination of the gain schedules learned in both the 4-1-4 and 10-10-10 networks reveals some peculiar properties. In particular, the gain in the last two time steps of the settling is much larger than in any of the other time steps. This effect is more apparent in the 4-1-4 networks and is believed to be caused by a combination of two factors:

1. The network architecture.
2. The generation of an external error signal only after the network has settled.

In order to understand the effects of these factors, consider figure 7-7, which presents a view of a 4-1-4 network exploded in time. Each row of the figure represents the state of a network at a point in time, the distance between rows representing a single time step. The bottom row is the beginning of a settling and the top row represents the end of the settling. Going across a row we see that the 4-1-4 net can be considered as having 3 layers of units (input, hidden and output). During the settling, signals flow either along columns, for interconnected units in the same layer, or along the diagonals, for interconnected units in different layers. The *history* of the network is defined as the sequence of states the network goes through during a single settling. Thus there is a history entry for each row in figure 7-7. These histories are stored locally by each unit. The backward pass for an iterative net starts with the history entry for the final time step of the settling and propagates error gradients backwards toward the history entry for the first time step of the settling. If we consider each row of figure 7-7 as a history entry, with the entry for the first time step of the settling at the bottom, and that for the last at the top, then the backward pass starts at the top of the figure and works its way toward the bottom (i.e. in the direction opposite to that indicated by the arrows on the figure). As in the forward pass, signals only propagate vertically or along diagonals. It is important to note that signals moving along diagonals are moving both between physical layers and between time steps.

Consider again the exploded 4-1-4 network. Note that since the input units can only communicate with the output units through the middle layer of units, there will be a two time step propagation delay for signals to move between the input and output layers in both the forward and backward pass. As error gradients are propagated back to earlier history entries, the magnitudes are greatly reduced. In a network in which the actual output is compared to the desired output only during the last time step of the settling there is a large external error input introduced at this last time step. This error signal will propagate back to the input unit histories corresponding to the two time steps immediately prior to the final time step. For all history entries prior to these last two, the error gradients will be

¹²These results are slower than for a corresponding problem with a layered network. This is attributed to different values for α and a different set of input vectors.

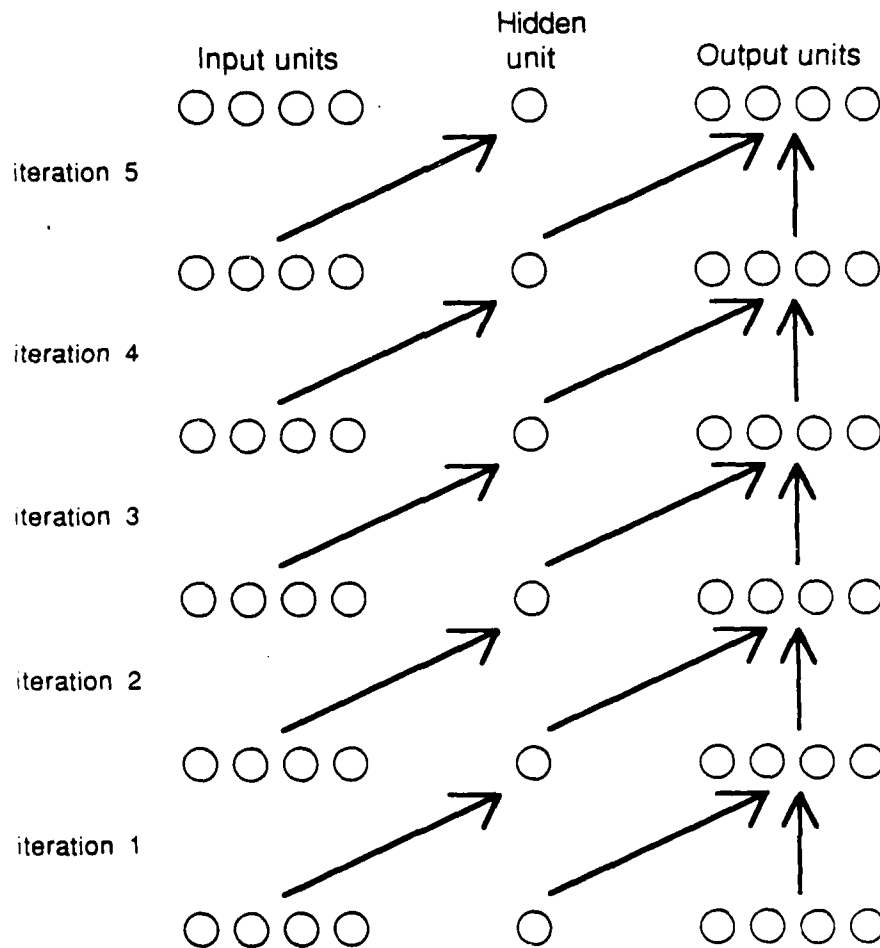


Figure 7-7: An exploded time view of a 4-1-4 network. Each row corresponds to a time step of the settling, with the bottom row being the beginning. Each arrow represents a set of connections.

residual error propagated back from error terms calculated for the last two time steps. These residual error gradients are smaller than the direct external errors. Recall that the gradient of the gain term is calculated by summing the gradients of all weights for each time step. The sum of the error gradients for the last two time steps will be much larger than for the other time steps. This will tend to drive the gain change more rapidly for these two steps, leading to the effect of much larger gains for these last two steps.

To test this hypothesis, two further groups of experiments were performed. In the first, a set of networks in which the propagation delays could be modified systematically were trained on a standard encoder problem. Each of these networks had 4 input units, 4 output units and n groups of 4 hidden units arranged so signals from the input units had to travel through all n groups of hidden units before reaching the output units. We call these 4- n 4-4 networks (see figure 7-8). If the propagation delays through the network affected the gain gradients as suggested then there

should be a linear relationship between the number of groups of hidden units and the number of time steps with large gains. Such a relationship was found for $n=1$ to 4. In general, if there were n groups of hidden units then the last n time steps all had gains larger than the other time steps. As n was increased this step effect in gain became less pronounced.

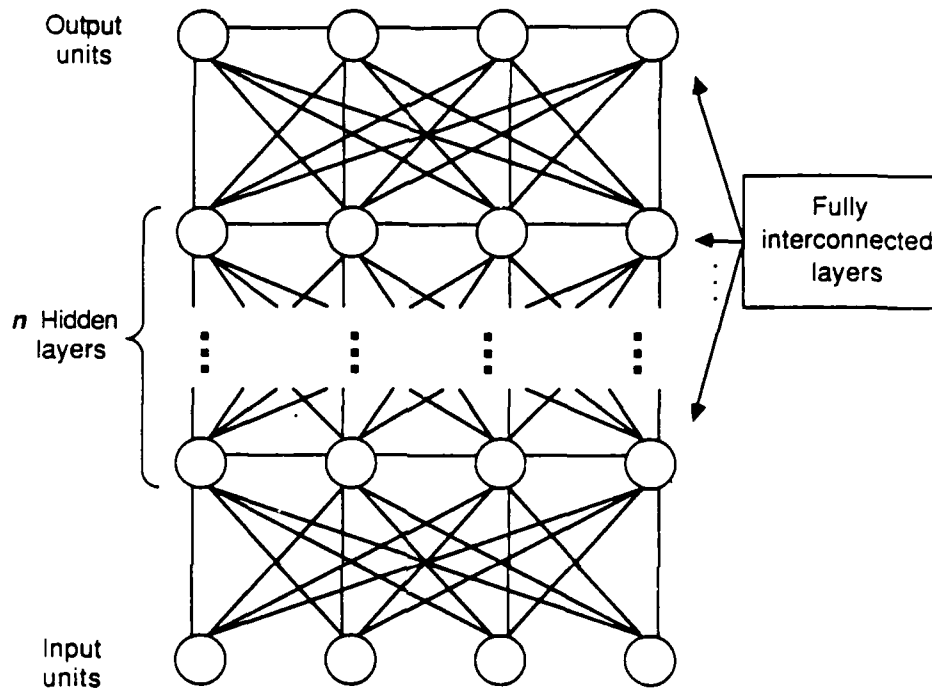


Figure 7-8: A 4- n -4 network.

The second group of experiments used a task in which the error for the output units was not always calculated during the final time step. The network consisted of 10 input units, 5 hidden units and a single output unit. Each hidden unit was connected to all 10 input units and also to the other 4 hidden units. The output unit was only connected to the 5 hidden units. The task the network had to learn required setting the state of the output unit to be 1 after a certain delay from the time the network started to settle. Each input unit corresponded to one of 10 different required delays, and only one input unit was on at a time. Since in this task the external error signals were well distributed over all of the time steps, there should be no sudden step towards the end of the settling process. The gain variation schedule learned for this problem showed no step in the gain response, as expected (see figure 7-9). However the gain schedule also did not exhibit the characteristic increase of gain over the settling period. Rather the gain tended to peak then decay during the settling period.

All of the results discussed in this section have been based on networks with asymmetric connections. The results

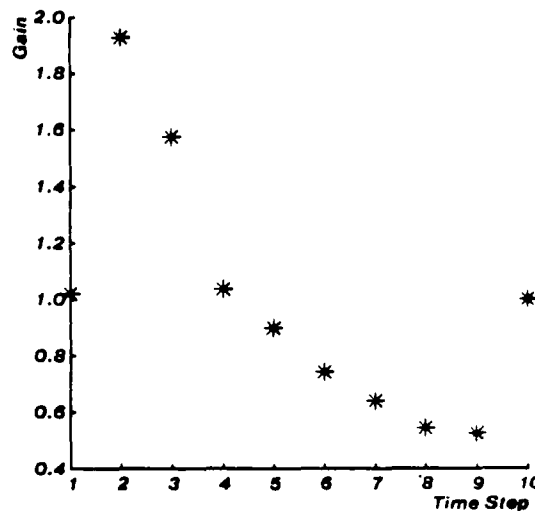


Figure 7-9: Gain schedule for the variable delay task.

of Hopfield and Tank [Hopfield 85], which this work has extended, were based on symmetric networks that have an energy function which governs their settling behavior. We investigated the effects of symmetrical connections by repeating the 4-1-4 encoder and 10-10-10 association problems using networks with symmetric connections. The results for the symmetric networks were identical to the results obtained for the asymmetric networks in terms of the effects of gain variation. It was noted that the symmetric networks required more epochs to learn the same tasks. This may be due to the greater number of connections and correspondingly higher fan-in for each unit (see Section 4), rather than a direct result of symmetry.

Several other experiments were performed to compare the performance of the learned gain schedules to schedules designed by hand. The schedules investigated provided linear, quadratic and exponential growth in gain over the settling period of a 4-1-4 encoder. None of these hand-tooled schedules could outperform the learned schedules, and most did not perform as well. The performance of these prespecified schedules varied from test case to test case, although both the quadratic and exponential schedules consistently outperformed the linear schedule. When any of these schedules were reversed so that gain tended to decrease during the settling the learning performance was degraded severely. In particular, the learning procedure became prone to becoming stuck in sub-optimal states, and often would become unstable and cease to converge on a solution, by moving in directions which led to increases in the error criterion.¹³

These experimental results support the view that gain variation can improve the performance of iterative networks. However, it is also apparent that the degree of improvement is problem dependent. Further research is

¹³Similar behavior is sometimes noted when weight decay is applied to a network.

required to determine which characteristics of a problem (and the associated state space) indicate that a problem can benefit substantially from gain variation.

References

- [Ackley 85] Ackley D.H., Hinton G.E. and Sejnowski T.J.
A learning algorithm for Boltzmann Machines.
Cognitive Science 9(2):147-169, 1985.
- [Feldman 82] Feldman J.A. and Ballard D.H.
Connectionist models and their properties.
Cognitive Science 6:205-254, 1982.
- [Hinton 83] Hinton G.E. and Sejnowski T.J.
Optimal perceptual inference.
In *Proceedings, IEEE conference on Computer Vision and Pattern Recognition*. Washington DC, June, 1983.
- [Hopfield 82] Hopfield J.J.
Neural networks and physical systems with emergent collective computational abilities.
Proceedings of the National Academy of Sciences 79:2554-2558, 1982.
- [Hopfield 85] Hopfield J.J. and Tank D.W.
"Neural" computation of decisions in optimization problems.
Biological Cybernetics 52:141-152, 1985.
- [Kirkpatrick 83] Kirkpatrick S., Gelatt C.D. and Vecchi M.P.
Optimization by simulated annealing.
Science 220:671-680, 1983.
- [Le Cun 85] Le Cun Y.
Une prodedure d'apprentissage pour reseau a seuil assymetrique (A learning scheme for asymmetric threshold network).
In *Cognitiva 85*. Paris, France, June, 1985.
- [Le Cun 86] Le Cun Y.
Learning process in an asymmetric threshold network.
In E. Bienenstock, F. Fogelman and G. Weisbuch (editors), *Disordered systems and biological organization*. Springer Verlag, New York, 1986.
- [Rumelhart 86] Rumelhart D.E., Hinton G.E. and Williams R.J.
Learning internal representations by error propagation.
In D.E. Rumelhart, J.L. McClelland and the PDP research group (editors), *Parallel distributed processing: Explorations in the microstructure of cognition. Volume I: Foundations*. MIT Press, Cambridge, MA, 1986.
- [Torre 86] Torre V. and Poggio T.A.
On edge detection.
IEEE Transactions on Pattern Analysis and Machine Intelligence PAMI-8(2):147-163, March, 1986.

1986/03/20

Distribution List [UCSD/Elman & McClelland] NR 667-483

Dr. Phillip L. Acherman
University of Minnesota
Department of Psychology
Minneapolis, MN 55455

Air Force Human Resources Lab
AFHRL/HRD
Brooks AFB, TX 78235

AFOSR,
Life Sciences Directorate
Bolling Air Force Base
Washington, DC 20332

Dr. Robert Ahlers
Code M711
Human Factors Laboratory
NAVTRAEQUIPCEN
Orlando, FL 32813

Dr. Ed Aiken
Navy Personnel R&D Center
San Diego, CA 92152

Dr. Earl A. Alluisi
HQ, AFHRL (AFSC)
Brooks AFB, TX 78235

Dr. James Anderson
Brown University
Center for Neural Science
Providence, RI 02912

Dr. John R. Anderson
Department of Psychology
Carnegie-Mellon University
Pittsburgh, PA 15213

Dr. Nancy S. Anderson
Department of Psychology
University of Maryland
College Park, MD 20742

Technical Director, ARI
5001 Eisenhower Avenue
Alexandria, VA 22333

Dr. Alan Baddeley
Medical Research Council
Applied Psychology Unit
15 Chaucer Road
Cambridge CB2 2EP
ENGLAND

Dr. Jackson Beatty
Department of Psychology
University of California
Los Angeles, CA 90024

Dr. Alvah Bittner
Naval Biodynamics Laboratory
New Orleans, LA 70189

Dr. John Black
Yale University
Box 11A, Yale Station
New Haven, CT 06520

Dr. Arthur S. Blalives
Code M711
Naval Training Equipment Center
Orlando, FL 32813

Dr. Gordon H. Bover
Department of Psychology
Stanford University
Stanford, CA 94306

Dr. Robert Breaux
Code N-095R
NAVTRAEQUIPCEN
Orlando, FL 32813

Dr. Gail Carpenter
Northeastern University
Department of Mathematics, 504LA
360 Huntington Avenue
Boston, MA 02115

Dr. Pat Carpenter
Carnegie-Mellon University
Department of Psychology
Pittsburgh, PA 15213

Chair, Department of
Psychology
College of Arts and Sciences
Catholic University of
America
Washington, DC 20064

Dr. Fred Chang
Navy Personnel R&D Center
Code 51
San Diego, CA 92152

Dr. David E. Clement
Department of Psychology
University of South Carolina
Columbia, SC 29208

Dr. Charles Clifton
Tobin Hall
Department of Psychology
University of
Massachusetts
Amherst, MA 01003

Dr. Michael Coles
University of Illinois
Department of Psychology
Champaign, IL 61820

Dr. John J. Collins
Director, Field Research
Office, Orlando
NPRDC Liaison Officer
NTSC Orlando, FL 32813

Dr. Stanley Collyer
Office of Naval Technology
Code 222
800 N. Quincy Street
Arlington, VA 22217-5000

Dr. Leon Cooper
Brown University
Center for Neural Science
Providence, RI 02912

CAPT P. Michael Curran
Office of Naval Research
800 N. Quincy St.
Code 125
Arlington, VA 22217-5000

Bryan Dallman
AFHRL/LRT
Lowry AFB, CO 80230

Dr. Joel Davis
Office of Naval Research
Code 1141NP
800 North Quincy Street
Arlington, VA 22217-5000

Dr. R. K. Dismukes
Associate Director for Life
Science
AFOSR
Bolling AFB
Washington, DC 20332

Dr. Emanuel Donchin
University of Illinois
Department of Psychology
Champaign, IL 61820

Defense Technical
Information Center
Cameron Station, Bldg 5
Alexandria, VA 22314
Attn: TC
(12 Copies)

Dr. Ford Ebner
Brown University
Anatomy Department
Medical School
Providence, RI 02912

Dr. Jeffrey Elman
University of California,
San Diego
Department of Linguistics, C-008
La Jolla, CA 92093

Dr. William Epstein
University of Wisconsin
V. J. Brogden Psychology Bldg.
1202 W. Johnson Street
Madison, WI 53706

ERIC Facility-Acquisitions
4833 Rugby Avenue
Bethesda, MD 20014

Dr. K. Anders Ericsson
University of Colorado
Department of Psychology
Boulder, CO 80309

Dr. W. E. Evans
Hubbs Sea World Institute
1720 S. Shores Rd.
Mission Bay
San Diego, CA 92109

1986/03/20

Distribution List [UCSD/Elman & McClelland] NR 667-483

1986/03/20

Distribution List [UCSD/Eiman & McClelland] NR 667-483

Dr. Martha Farah
Department of Psychology
Carnegie-Mellon University
Schenley Park
Pittsburgh, PA 15213

Dr. Jerome A. Feldman
University of Rochester
Computer Science Department
Rochester, NY 14627

J. D. Fletcher
9931 Corsica Street
Vienna VA 22180

Dr. John B. Frederiksen
Bolt Beranek & Newman
50 Moulton Street
Cambridge, MA 02138

Dr. Michaela Gallagher
University of North Carolina
Department of Psychology
Chapel Hill, NC 27514

Dr. Michael Genesereth
Stanford University
Computer Science Department
Stanford, CA 94305

Dr. Don Gentner
Center for Human
Information Processing
University of California
La Jolla, CA 92093

Dr. Claude Ghez
Center for Neurobiology and
Behavior
722 W. 168th Street
New York, NY 10032

Dr. Gene L. Glove
Office of Naval Research
Detachment
1030 E. Green Street
Pasadena, CA 91106-2485

Dr. Sam Glucksberg
Princeton University
Department of Psychology
Green Hall
Princeton, NJ 08540

Dr. Daniel Gopher
Industrial Engineering
& Management
TECHNION
Haifa 32000
ISRAEL

Dr. Sherrill Gott
AFRL/MDJ
Brooks AFB, TX 78235

Jordan Grafman, Ph.D.
Department of Clinical
Investigation
Walter Reed Army Medical Center
6825 Georgia Ave., N. W.
Washington, DC 20307-5001

Dr. Richard B. Granger
Department of Computer Science
University of California, Irvine
Irvine, CA 92717

Dr. Wayne Gray
Army Research Institute
5001 Eisenhower Avenue
Alexandria, VA 22333

Dr. William Greenough
University of Illinois
Department of Psychology
Champaign, IL 61820

Dr. Stephen Grossberg
Center for Adaptive Systems
Room 244
111 Cummings Street
Boston University
Boston, MA 02215

Dr. Muhammad K. Habib
University of North Carolina
Department of Biostatistics
Chapel Hill, NC 27514

Dr. Henry M. Hallit
Hallit Resources, Inc.
4918 33rd Road, North
Arlington, VA 22207

Dr. Ray Hannapel
Scientific and Engineering
Personnel and Education
National Science Foundation
Washington, DC 20550

Stevan Harnad
Editor, The Behavioral and
Brain Sciences
20 Nassau Street, Suite 240
Princeton, NJ 08540

Dr. Steven A. Hillyard
Department of Neurosciences
University of California,
San Diego
La Jolla, CA 92093

Dr. Geoffrey Hinton
Carnegie-Mellon University
Computer Science Department
Pittsburgh, PA 15213

Dr. Jim Hollan
Intelligent Systems Group
Institute for
Cognitive Science (C-015)
UCSD
La Jolla, CA 92093

Dr. John Holland
University of Michigan
2313 East Engineering
Ann Arbor, MI 48109

Dr. Keith Holyoak
University of Michigan
Human Performance Center
330 Packard Road
Ann Arbor, MI 48109

Dr. Earl Hunt
Department of Psychology
University of Washington
Seattle, WA 98105

Dr. Alice Isen
Department of Psychology
University of Maryland
Catonsville, MD 21228

Chair, Department of
Psychology
The Johns Hopkins University
Baltimore, MD 21218

Dr. Marcel Just
Carnegie-Mellon University
Department of Psychology
Schenley Park
Pittsburgh, PA 15213

Dr. Daniel Kahneman
The University of British Columbia
Department of Psychology
#154-2053 Main Mall
Vancouver, British Columbia
CANADA V6T 1V7

Dr. Demetrios Karis
Grumman Aerospace Corporation
MS C04-14
Bethpage, NY 11714

Dr. Milton S. Katz
Army Research Institute
5001 Eisenhower Avenue
Alexandria, VA 22333

Dr. Steven V. Keele
Department of Psychology
University of Oregon
Eugene, OR 97403

Dr. Wendy Kellogg
IBM T. J. Watson Research Ctr.
P.O. Box 218
Yorktown Heights, NY 10598

Dr. Scott Kelso
Haskins Laboratories,
270 Crown Street
New Haven, CT 06510

Dr. David Klahr
Carnegie-Mellon University
Department of Psychology
Schenley Park
Pittsburgh, PA 15213

1986/03/20

Distribution List [UCSD/Eiman & McClelland] NR 667-483

1986/03/20

Distribution List [UCSD/Elman & McClelland] NR 667 483

Dr. Sylvan Kornblum
University of Michigan
Mental Health Research Institute
205 Washtenaw Place
Ann Arbor, MI 48109

Dr. Stephen Kosslyn
Harvard University
1236 William James Hall
33 Kirkland St.
Cambridge, MA 02138

Dr. David R. Loeber
Naval Ocean Systems Center
Code 441T
271 Catalina Boulevard
San Diego, CA 92152

Dr. Pat Langley
University of California
Department of Information
and Computer Science
Irvine, CA 92717

Dr. Mancy Lansman
University of North Carolina
The L. L. Thurstone Lab.
Davis Hall 013A
Chapel Hill, NC 27514

Dr. Robert Lawler
Information Sciences, FRL
GTE Laboratories, Inc.
40 Sylvan Road
Waltham, MA 02254

Dr. Alan M. Lesgold
Learning R&D Center
University of Pittsburgh
Pittsburgh, PA 15260

Dr. Alan Leshner
Deputy Division Director
Behavioral and Neural Sciences
National Science Foundation
1800 G Street
Washington, DC 20550

Dr. Gary Lynch
University of California
Center for the Neurobiology of
Learning and Memory
Irvine, CA 92717

Dr. Don Lyon
P. O. Box 46
Higley, AZ 85236

Dr. James McBride
Psychological Corporation
c/o Marcourt, Brace,
Javanovich Inc.
1250 West 6th Street
San Diego, CA 92101

Dr. Jay McClelland
Department of Psychology
Carnegie-Mellon University
Pittsburgh, PA 15213

Dr. James L. McCaugh
Center for the Neurobiology
of Learning and Memory
University of California, Irvine
Irvine, CA 92717

Dr. Joe McLachlan
Navy Personnel R&D Center
San Diego, CA 92152

Dr. James McMichael
Assistant for MPT Research,
Development, and Studies
NAVOP 01B7
Washington, DC 20370

Dr. Al Meyrovitz
Office of Naval Research
Code 1133
800 N. Quincy
Arlington, VA 22217-5000

Dr. George A. Miller
Department of Psychology
Green Hall
Princeton University
Princeton, NJ 08540

Dr. Tom Moran
Xerox PARC
3133 Coyote Hill Road
Palo Alto, CA 94304

Chair, Department of
Computer Science
U.S. Naval Academy
Annapolis, MD 21402

1986/03/20

Distribution List [UCSD/Elman & McClelland] NR 667 483

Chair, Department of
Systems Engineering
U.S. Naval Academy
Annapolis, MD 21402

Dr. David Navon
Institute for Cognitive Science
University of California
La Jolla, CA 92093

Dr. Allen Nevell
Department of Psychology
Carnegie-Mellon University
Schenley Park
Pittsburgh, PA 15213

Dr. Mary Jo Nissen
University of Minnesota
N218 Elliott Hall
Minneapolis, MN 55455

Dr. Donald A. Norman
Institute for Cognitive Science
University of California
La Jolla, CA 92093

Director, Training Laboratory,
NPRDC (Code 05)
San Diego, CA 92152

Director, Manpower and Personnel
Laboratory,
NPRDC (Code 06)
San Diego, CA 92152

Director, Human Factors
& Organizational Systems Lab,
NPRDC (Code 07)
San Diego, CA 92152

Fleet Support Office,
NPRDC (Code 301)
San Diego, CA 92152

Library, NPRDC
Code P7011
San Diego, CA 92152

Dr. Stellan Ohlsson
Learning R & D Center
University of Pittsburgh
3939 O'Hara Street
Pittsburgh, PA 15213

Office of Naval Research,
Code 1133
800 N. Quincy Street
Arlington, VA 22217-5000

Office of Naval Research,
Code 1141NP
800 N. Quincy Street
Arlington, VA 22217-5000

Office of Naval Research,
Code 1142EP
800 N. Quincy Street
Arlington, VA 22217-5000

Office of Naval Research,
Code 1142PT
800 N. Quincy Street
Arlington, VA 22217-5000
(6 Copies)

Psychologist
Office of Naval Research
Branch Office, London
Box 39
FPO New York, NY 09510

Special Assistant for Marine
Corps Matters,
ONR Code 09MC
800 N. Quincy St.
Arlington, VA 22217-5000

Psychologist
Office of Naval Research
Liaison Office, Far East
APO San Francisco, CA 96303

Dr. Judith Orasanu
Army Research Institute
5001 Eisenhower Avenue
Alexandria, VA 22333

Daira Paulson
Code 52 - Training Systems
Navy Personnel R&D Center
San Diego, CA 92152

Dr. James V. Pellegrino
University of California,
Santa Barbara
Department of Psychology
Santa Barbara, CA 93106

1986/03/20

Distribution List [UCSD/Elsan & McClelland] NR 667-483

Department of Computer Science,
Naval Postgraduate School
Monterey, CA 93940

Dr. Steven Pinker
Department of Psychology
810 018
M.I.T.
Cambridge, MA 02139

Dr. Martha Polson
Department of Psychology
Campus Box 346
University of Colorado
Boulder, CO 80309

Dr. Peter Polson
University of Colorado
Department of Psychology
Boulder, CO 80309

Dr. Mike Posner
University of Oregon
Department of Psychology
Eugene, OR 97403

Dr. Karl Pribram
Stanford University
Department of Psychology
Bldg. 4201 -- Jordan Hall
Stanford, CA 94305

Dr. Lynne Reder
Department of Psychology
Carnegie Mellon University
Schenley Park
Pittsburgh, PA 15213

Dr. James A. Reggia
University of Maryland
School of Medicine
Department of Neurology
22 South Greene Street
Baltimore, MD 21201

Dr. Daniel Reisberg
Department of Psychology
New School for Social Research
65 Fifth Avenue
New York, NY 10003

Dr. Gill Ricard
Mail Stop CD4-14
Grumman Aerospace Corp.
Bethpage, NY 11714

Dr. David Rumelhart
Center for Human
Information Processing
Univ. of California
La Jolla, CA 92093

Dr. E. L. Saltzman
Haskins Laboratories
270 Crown Street
New Haven, CT 06510

Dr. Arthur Samuel
Yale University
Department of Psychology
Box 11A, Yale Station
New Haven, CT 06520

Dr. Robert Sasmor
Army Research Institute
5001 Eisenhower Avenue
Alexandria, VA 22333

Dr. Walter Schneider
Learning R&D Center
University of Pittsburgh
3939 O'Hara Street
Pittsburgh, PA 15260

Dr. Hans-Villi Schroiff
Institut fuer Psychologie
der RWTH Aachen
Jaegerstrasse zwischen 17 u. 19
5100 Aachen
WEST GERMANY

Dr. Marc Sebrechts
Department of Psychology
Wesleyan University
Middletown, CT 06475

Dr. T. B. Sheridan
Dept. of Mechanical Engineering
MIT
Cambridge, MA 02139

1986/03/20

Distribution List [UCSD/Elsan & McClelland] NR 667-483

Dr. Randall Shumaker
Naval Research Laboratory
Code 7510
4555 Overlook Avenue, S.W.
Washington, DC 20375-5000

Dr. Miriam Schustack
Code 51
Navy Personnel R & D Center
San Diego, CA 92152

Dr. Herbert A. Simon
Department of Psychology
Carnegie Mellon University
Schenley Park
Pittsburgh, PA 15213

Dr. Kathryn T. Spoeher
Brown University
Department of Psychology
Providence, RI 02912

Dr. Ted Steinke
Dept. of Geography
University of South Carolina
Columbia, SC 29208

Dr. Saul Sternberg
University of Pennsylvania
Department of Psychology
3815 Walnut Street
Philadelphia, PA 19104

Dr. Paul J. Sticha
Senior Staff Scientist
Training Research Division
HumRRO
1100 S. Washington
Alexandria, VA 22314

Dr. John Tangney
AFOSR/NL
Boiling AFB, DC 20332

Dr. Richard F. Thompson
Stanford University
Department of Psychology
Bldg. 4201 Jordan Hall
Stanford, CA 94305

Dr. Michael T. Turvey
Haskins Laboratories
270 Crown Street
New Haven, CT 06510

Dr. James Tweeddale
Technical Director
Navy Personnel R&D Center
San Diego, CA 92152

Headquarters, U. S. Marine Corps
Code MP1-20
Washington, DC 20380

Dr. William Uttal
NOSC, Hawaii Lab
Box 997
Kailua, HI 96734

Dr. Kurt Van Lehn
Department of Psychology
Carnegie-Mellon University
Schenley Park
Pittsburgh, PA 15213

Dr. Beth Varten
Bolt Beranek & Newman, Inc.
50 Moulton Street
Cambridge, MA 02138

Dr. Shih-Sung Ven
Jackson State University
1325 J. R. Lynch Street
Jackson, MS 39217

Dr. Douglas Wetzel
Code 12
Navy Personnel R&D Center
San Diego, CA 92152

Dr. Barry Whitset
University of North Carolina
Department of Physiology
Medical School
Chapel Hill, NC 27514

Dr. Christopher Wickens
Department of Psychology
University of Illinois
Champaign, IL 61820

1986/03/20

Distribution List [UCSD/Elman & McClelland] NR 667-483

Dr. Robert A. Wisner
U.S. Army Institute for the
Behavioral and Social Sciences
5001 Eisenhower Avenue
Alexandria, VA 22333

Dr. Donald Woodward
Office of Naval Research
Code 1141NP
800 North Quincy Street
Arlington, VA 22217-5000

Dr. Wallace Wulfeck, III
Navy Personnel R&D Center
San Diego, CA 92152

Dr. Joe Yasutake
AFHRL/LRT
Lowry AFB, CO 80230

Mr. Carl York
System Development Foundation
181 Lytton Avenue
Suite 210
Palo Alto, CA 94301

Dr. Joseph L. Young
Memory & Cognitive
Processes
National Science Foundation
Washington, DC 20550

Dr. Steven Zornetzer
Office of Naval Research
Code 1140
800 N. Quincy St.
Arlington, VA 22217-5000

Dr. Michael J. Zyda
Naval Postgraduate School
Code 520K
Monterey, CA 93943

DATE
FILMED
6-8